Cardiomyocyte-specific deletion of β-catenin protects mouse hearts from ventricular arrhythmias after myocardial infarction

By: Jerry Wang

M.Sc. Candidate

This thesis is submitted to the University of Ottawa

in partial fulfillment of the requirements for the Degree of:

Master of Science in Cellular and Molecular Medicine

Department of Cellular and Molecular Medicine

Faculty of Medicine

University of Ottawa

University of Ottawa Heart Institute

Abstract

Wnt/β-catenin signaling is activated in the heart after myocardial infarction (MI). This study aims to investigate if β-catenin deletion affects post-MI ion channel gene alterations and ventricular tachycardias (VT). MI was induced by permanent ligation of left anterior descending artery in wild-type (WT) and cardiomyocyte-specific β-catenin knockout (KO) mice. KO mice showed reduced susceptibility to VT (18% vs. 77% in WT) at 8 weeks after MI, associated with reduced scar size and attenuated chamber dilation. qPCR analyses of both myocardial tissues and purified cardiomyocytes demonstrated upregulation of Wnt pathway genes in border and infarct regions after MI, including Wnt ligands (such as *Wnt4*) and receptors (such as *Fzd1* and *Fzd2*). At 1 week after MI, cardiac sodium channel gene (*Scn5a)* transcript was reduced in WT but not in KO hearts, consistent with previous studies showing *Scn5a* inhibition by Wnt/β-catenin signaling. At 8 weeks after MI when Wnt genes have declined, *Scn5a* returned to near sham levels and K^+ channel gene downregulations were not different between WT and KO mice. This study demonstrated that VT susceptibility in the chronic phase after MI is reduced in mice with cardiomyocyte-specific β-catenin deletion primarily through attenuated structural remodeling, but not ion channel gene alterations.

ii. Acknowledgements

Firstly, I would like to thank my supervisors Dr. Wenbin Liang and Dr. Rob Beanlands for their excellent mentorship, guidance, and support. Both supervisors are great scientists who are also very capable team leaders, and truly helped me grow both academically and individually. My time in the lab and as part of the research group has been very enriching and fulfilling, and I have gained a wealth of knowledge and experimental techniques that are sure to help me succeed wherever life takes me.

I also thank the various members of the lab, but especially Dr. Alice Lu, our Postdoctoral Fellow, for being a great mentor and friend. Alice guided me through my first years of basic research, where she trained me from the ground up in nearly all my experimental techniques. Thank you as well to Ying Xia and Dr. Hongwei Wang for their assistance with various experiments crucial to the completion of this project. I am so thankful that you both joined the lab part way through my training, as we each had our own area of expertise to share and bring to the team.

A huge thank you to my thesis advisory committee, Dr. Peter Liu and Dr. Darryl Davis for your extremely helpful comments, suggestions, and help offered throughout my project. You each brought deep understanding of different perspectives which really helped round out my own research and greatly contributed to the project in its final form below.

Finally, I would like to thank my amazing friends and family. Thank you, mom and dad, for always supporting me 110% and bringing out the best in me. Thank you to all my friends both new and old, in and outside of the lab. And special thanks to Chloe for keeping me company, helping me drastically improve my presentations, and editing various applications and texts throughout my master's degree.

iii. List of Contributions

Lab training was provided by various lab members, while experiments were primarily performed by Jerry Wang with assistance from Dr. Alice Lu, Dr. Hongwei Wang, Ying Xia, and the supervisors. The funding of this project was made possible by the supervisors and the University of Ottawa Heart Institute Endowed Graduate Award. Both supervisors were responsible for the conception and design of this project. Animal surgeries and operations were performed by Dr. Alice Lu, while the University of Ottawa Animal Care and Veterinary Service team was responsible for the day-to-day care and maintenance of all animals used in this project.

iv. List of Abbreviations

Beta-catenin	β-catenin
Cardiovascular Disease	CVD
Ejection Fraction	EF
Electrocardiogram	ECG
End Diastolic Volume	EDV
End Systolic Volume	ESV
Frizzled	FZD
Left Coronary Artery	LCA
Heart Failure	HF
Left Ventricle	LV
Left Ventricular Internal Diameter at Diastole	LVIDd
Left Ventricular Internal Diameter at Systole	LVIDs
Left Ventricular Posterior Wall thickness at Diastole	LVPWd
Left Ventricular Posterior Wall thickness at Systole	LVPWs
Myocardial Infarction	MI
Myosin Heavy Chain, α-isoform	αMHC
Programmed Electrical Stimulation	PES
Sudden Cardiac Death	SCD
Ventricular Fibrillation	VF
Ventricular Tachycardia	VT
Wingless/Integrated	Wnt

1. Introduction

1.1 Cardiovascular Disease

Cardiovascular disease (CVD) remains the leading cause of death globally, despite continued advances in health care and interventions (World Health Organization, 2019). Of the various conditions encompassed by CVDs, ischemic heart disease, especially myocardial infarction (MI) also commonly known as a heart attack, is the most common. In MI, occlusion of a coronary artery results in the stoppage of blood flow to the corresponding region of the heart, which in turn causes lack of oxygen and nutrient supply, leading to tissue damage and death (Libby, 2005; Reed, 2017). The heart possesses some capacity for repair after an MI, but the process is inefficient and results in adverse remodeling with loss of normal cardiac structure and function. Despite current MI therapies including invasive coronary interventions and antithrombotic agents, patients with a history of MI have a high risk of ventricular arrhythmias which has been linked to a 6-fold increase in mortality post-MI (Henkel, 2006; Bhar-Amato, 2017). Sudden cardiac death resulting from arrhythmias is responsible for 15-20% of all mortality worldwide (Adabag, 2010; Srinivasen, 2018).

1.2 Arrhythmias in Cardiovascular Disease

The 2-year mortality of post-MI patients is estimated at 25-50%, and about half of these cases are due to sudden cardiac death, secondary to sustained ventricular tachycardia (VT) or ventricular fibrillation (VF) (Bhar-Amato, 2017; Bui, 2018). The increased risk of arrhythmia is attributable to several potential arrhythmia substrates which can be a result of either the structural remodeling, or the electrical remodeling which occurs in post-MI heart failure (HF) (Burchfield, 2013). Fibrosis occurs during the cardiac remodeling process, wherein extracellular

matrix is deposited to replace dead myocardium, but this leads to contractile dysfunction and complications with electrical conduction (Spinale, 2017). Another potential source of arrhythmia substrate is the dysregulation of myocyte ion channels and ion transporter proteins. Studies have shown that gap junction protein (Connexin43) distribution in post-MI myocytes occurs diffusely across the cell membrane, instead of its usual localization solely at intercalated disks between myocytes (Wit, 2012). Cardiac ion channels may also be grossly dysregulated, with numerous studies showing alterations in cardiac sodium channels: $Na_v1.5$ (Pu, 1997; Undrovinas, 1999; Huang, 2001; Maltsev, 2007), sodium-calcium exchanger (Pogwizd, 2001; Wang, 2010), L-type calcium current (Pitt 2006, Wang, 2008), and both inward and outward potassium currents (Kääb, 1998; Pogwizd 2001; Tsuji, 2000). Related to ion channel remodeling is the presence of reentry circuits due to small bundles or regions of surviving myocytes and purkinje fibers in the scar with altered electrophysiological properties. Their action potential durations (APDs), reduced maximal upstroke velocity (V_{max}), and more depolarized resting membrane potential (E_m) are further potential sources for the arrhythmia substrate (Gorenek, 2015).

The current clinical landscape for post-MI patients involves the implantable cardioverter-defibrillator (ICD), which can prevent the occurrence of VT/VF. However, previous clinical studies also found that implantation of the ICD too soon after MI increased MI (Hohnloser, 2009; Steinbeck, 2009). Additionally, pharmacological treatments which targeted the occurrence of frequent premature ventricular contractions (PVCs) following MI were found to reduce PVC frequency, but also increased mortality (CAST Investigators, 1989). There is a window of vulnerability following an MI where patients with and without revascularization are at increased risk of SCD due to arrhythmias.

Arrhythmias post-MI occur because of the ischemic region developing hypoxia. As oxygen levels deplete, intracellular metabolism switches to anaerobic glycolysis, causing a drop in pH, which leads to calcium overload due to the activation of Na^+/H^+ and Na^+/Ca^{2+} exchange (Diego, 2011). Extracellular potassium accumulates, the resting membrane potential is more depolarized, and conduction velocity is decreased (Gorenek, 2015). All these factors combine to greatly increase the risk of developing arrhythmias and contribute to maintaining arrhythmias that arise.

The three main categories of underlying cause for arrhythmia are automaticity, triggered activity, and reentry. Automaticity arrhythmias involve myocardial stretch-related injuries which can affect the tissue around the sinus node, causing spontaneous depolarizations near the pacemaker node. Triggered activity arrhythmias arise from Purkinje fibers and/or cardiomyocytes undergoing Ca^{2+} overload. Finally, reentry occurs when the ventricular wave front hits a region with unidirectional block, propagating along atypical pathways which can re-excite an area upstream, resulting in sustained reentrant impulses. (Janse, 1989; Pogwizd, 1990; Janse, 2003).

The most common arrhythmia substrate for VT in post-MI myocardium is a reentry circuit formed by surviving bundles of purkinje fibers and cardiomyocytes within the scar tissue (Marchlinski, 1983). The slowed conduction velocity and unidirectional block in scar and border zone tissue create the storm of conditions to support a reentrant and sustained VT, which can evolve to VF (Mont, 1996). This increased incidence of VT and VF is what is responsible for the greatly elevated risk and mortality due to SCD in post MI patients, and why managing these arrhythmias is so crucial (Bhar-Amato, 2017).

1.3 Wnt signaling

The Wnt signaling pathways are evolutionarily conserved and are involved in numerous cellular processes, playing a large role in development by influencing cellular proliferation, polarity, migration, and differentiation (Eberhart, 2001; Dawson, 2013; Steinhart, 2018). The Wnt signaling pathways involve the binding of Wnt ligands from the extracellular space to their receptors on the plasma membrane, including Frizzled (Fzd) receptors and various co-receptors, such as Low-Density Lipoprotein Receptor Related Protein 5/6 (LRP5/6), Receptor Tyrosine Kinase Like Orphan Receptor 1/2 (ROR1/2), and Related to Tyrosine Kinase (Ryk/Derailed). In total, there are 19 different Wnt ligands and 10 Fzd receptors expressed in mammals (Dawson, 2013).

The Wnt ligands are extracellular-secreted ligands. After being synthesized in the ER, they require essential modification by the acyltransferase Porcupine, and glycosylation, before being secreted. Each Wnt ligand has different properties and each Wnt ligand can bind to specific Fzd receptors, and vice-versa. The signaling pathway activated by the binding of a Wnt ligand to a Fzd receptor also depends on the particular ligand, receptor, and other cellular contexts (Nusse, 2006). However, all Wnt ligands do share a specific cysteine residue orientation which form disulfide bridges and confer their globular secondary structure (Willert, 2012).

1.4 Canonical/β-catenin Dependent Wnt Signaling

The β-catenin dependent pathway, also known as the canonical Wnt pathway, is one of the most important developmental pathways throughout the entire animal kingdom. Initially discovered in Drosophila, the Canonical Wnt pathway is characterized by cytosolic accumulation of β-catenin and its subsequent nuclear translocation.

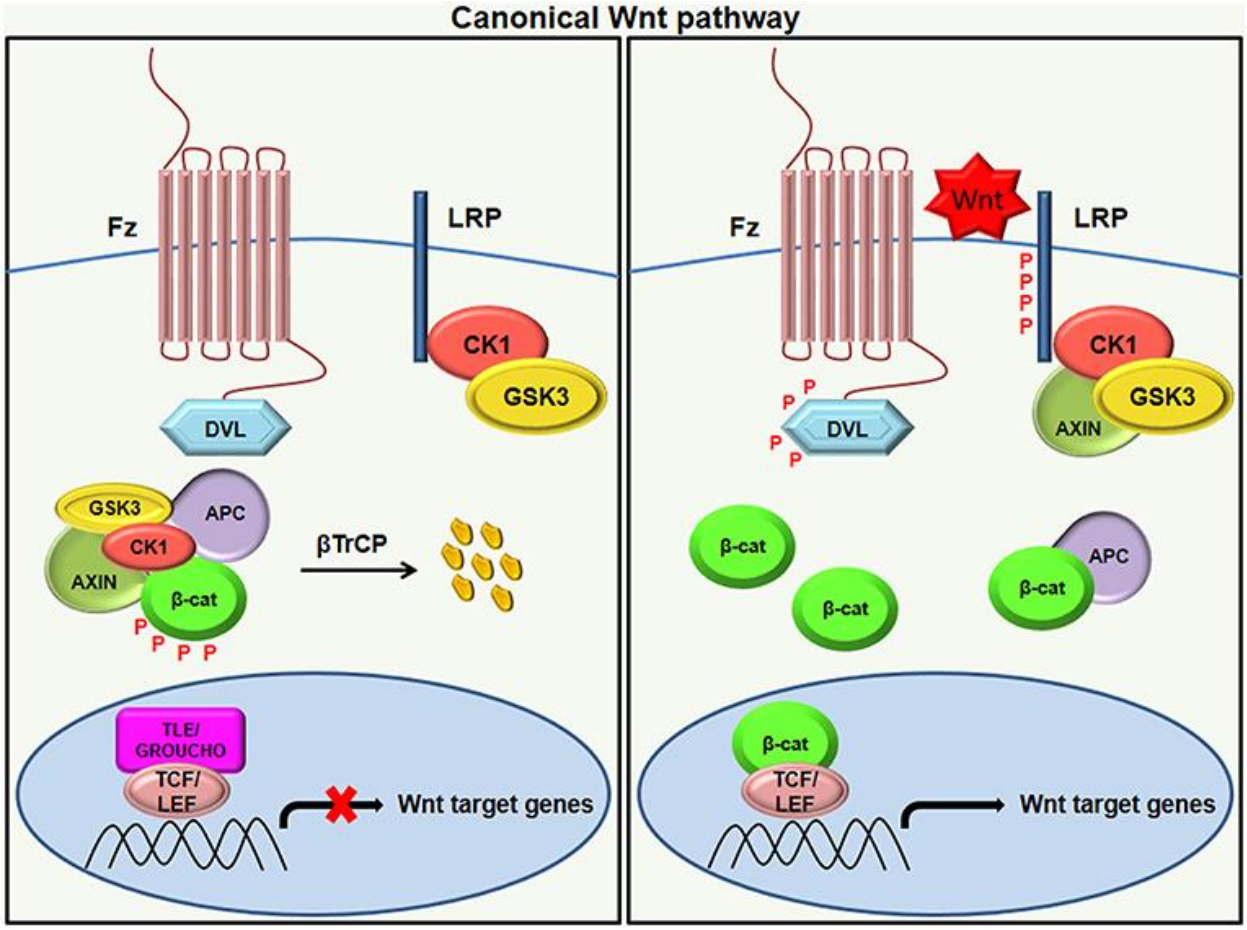

Figure i. Schematic of the Canonical Wnt signaling pathway. In the inactivated, Wnt ligand absent state (left), β-catenin is phosphorylated by the β-catenin destruction complex (composed of axin, APC, CK1, and the key component GSK3β), leading to its ubiquitination by Beta-Transducin repeats containing protein (β-TrCP), and eventual proteasomal degradation. Without nuclear accumulation of β-catenin, a repressor complex (containing TCF/LEF and corepressors TLE/Groucho) binds to the Wnt target genes and represses their activity. Wnt ligand presence in the extracellular domain eventually results in its binding to the Frizzled receptor and LRP co-receptor (right), which recruits Dishevelled (Dvl) proteins to the plasma membrane from the nucleus. This leads to LRP receptor phosphorylation by the kinases CK1 and GSK3β, inhibiting the β-catenin destruction complex and destruction of cytosolic β-catenin. β-catenin then accumulates in the cytoplasm and is translocated to the nucleus, where it binds to its partners

(such as TCF/LEF) and induces transcription of Wnt pathway target genes. (Figure from Patel, 2019)

In the absence of canonical Wnt ligands, a constitutively active system containing Glycogen synthase kinase-3 (GSK-3β) with Adenomatosis Polyposis Coli (APC), Axin, and Casein Kinase 1α (CK1), destroys cytosolic β-catenin through rapid GSK-3β phosphorylation of β-catenin. This targeted destruction occurs when GSK3β, along with its casein kinase partner CK1, phosphorylate three specific serine residues – Ser45 by CK1, then Ser33, Ser37, and Thr41 by GSK3β (Liu, 2002; Xing, 2003). The phosphorylation of these sites allows β-TrCP to recognize the phospho-sites and recruit a ubiquitination complex to ubiquitinate β-catenin, leading to its degradation by the 26S proteasome (Hart, 1999). Axin contributes to the destruction complex and degradation of β-catenin by increasing GSK3β's kinase activity (Dajani, 2003). APC is also a critical component of the complex since it stabilizes the phosphorylated residues of β-catenin. Without APC-β-catenin interaction, β-catenin is instead dephosphorylated by PP2A, and subsequently cannot be recognized and ubiquitinated by β-TrCP (Su, 2008).

When Wnt ligands are present, binding to and activation of FZD receptors causes Axin to translocate to the cell membrane and bind to the intracellular domain of LRP5/6, which in turn leads to the phosphorylation and activation of Dishevelled (Dvl) protein (Mao, 2011; Zeng, 2008). Dvl inhibits GSK-3β activity by binding to Axin and GSK-3β, disrupting the destruction complex (Gordon, 2006; Hatsell, 2008). This leads to ß-catenin stabilization (non-phosphorylation), accumulation in the cytosol, and its subsequent translocation into the nucleus where, together with members of the T-cell factors (TCF)/lymphoid enhancer-binding factor (LEF) family, they regulate transcription of target genes through binding of promotor domains (Habas, 2005; Kikuchi, 2009). Until very recently, the translocation of β-catenin into the nucleus

was poorly understood, since β-catenin itself does not have a nuclear localization sequence, nor has there been any evidence to show involvement with previously studied importin proteins or other nuclear import mechanisms like the Ran-GEF system (Fagotto, 1998; Qi, 2006; Komiya, 2008). However, a recent study demonstrated in *Xenopus* that the molecular mechanism for β-catenin nuclear translocation involves the GTP-bound activation of nuclear GTPases (Rap1a/b) by the protein RAPGEF5, in an energy-dependent manner that mimics Ran-GEF transport but utilizes a different set of molecular machinery (Griffin, 2019). Once β-catenin has entered the nucleus, it acts as a transcriptional co-activator and occasionally co-repressor alongside many binding partners, before being exported and finally degraded.

Wnt/β-catenin signaling is a critical component of embryonic development. The signaling cascades triggered are extremely sensitive and act in a gradient mechanism, governing both the body's dorsoventral axis, and anteroposterior axis development (Gomez, 2008; Niehrs, 2010; Janssen, 2010). Wnt/β-catenin signaling is also one of a trio of signaling pathways, including leukemia inhibitory factor signaling and MAPK pathway inhibition, which maintains the naïve state of pluripotent stem cells (Lyashenko, 2011), both in the embryonic stage and in adult homeostasis of various tissues, including the gut (Barker, 2007), the stomach (Barker, 2010), the mammary gland (van Amerongen, 2012), the skin (Lim, 2013), and the liver (Wang, 2015). Since Wnt/β-catenin signaling is so involved in stem cell replication, disruption of the pathway, often via mutation of APC (Nishisho, 1991), a component of the destruction complex, is linked to cancers in the tissues above due to aberrant stabilization of β-catenin and increased signaling and downstream proliferation (Rubenfield, 1996).

1.5 β-catenin

β-catenin is an evolutionarily conserved protein with immense importance, playing crucial roles during development such as in cell-to-cell adhesion and in canonical Wnt signaling pathways. β-catenin's multiple roles in the cell arise from two main functions, 1) as a structural element, and 2) as a cellular signaling component of the canonical Wnt pathway, as described above.

The structure of the ~80-90kDa β-catenin protein confers its multifunctional abilities within the cell. The characteristic central region, composed of 12 Armadillo-repeats each forming a superhelix structure of three alpha helices, provides a strong, rigid backbone which supports the binding of many molecular partners at various locations within the repeats, both in the cytosol and in the nucleus (Huber, 1997; Xing, 2008). Between the last Armadillo repeat and the C-terminal domain (CTD) is a special helix, Helix-C, whose hydrophobic residues interact with and cap the hydrophobic residues on the end of the 12th Armadillo repeat (Xing, 2014). This helix has also been proven to play a key role in the signaling role of β-catenin, but no role for Helix-C has been found regarding the structural, adherens junction related role of β-catenin (Xing, 2008). Another key characteristic of β-catenin's partner-binding capacity is the overlapping of binding sites to its potential partners, ensuring that two partners for different pathways/functions cannot bind simultaneously – there is mutual exclusivity among β-catenin's binding partners (Graham, 2000; Huber and Weis, 2001).

Flanking the Armadillo repeats in the middle are the N-terminal domain (NTD) and the C-terminal domain (CTD). A key property of these two domains is that they are much more flexible than the Armadillo domain and can fold back onto the central region, also aiding or inhibiting the binding of other factors (Castano, 2002; Solanas, 2004). In fact, one group's biochemical evidence strongly suggests that β-catenin, when performing as a transcriptional mediator in the nucleus, is primarily in a monomeric, NTD and CTD back-folded form (Gottardi,

2004). This back-folded configuration helps β-catenin bind to its TCF/Lef partners by strengthening their interactions. However, when β-catenin is bound to cadherin in the cytoplasm, its structure becomes non-folded, and it dimerizes with α-catenin (Pokutta, 2000; Gottardi, 2004).

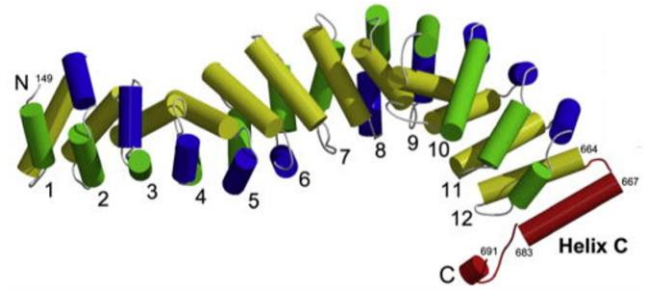

Figure ii. The crystal structure of β-catenin. The 12 Armadillo repeats, each containing three alpha helices (green, yellow, blue) arranged in a triangular formation, make up most of β-catenin's structure. Flanking the ends are the N-terminal domain and the C-terminal domain, along with an extra helix (red), Helix-C. (Figure from Xing, 2008)

The majority of cellular β-catenin is typically found as part of the adherens junction since free cytosolic β-catenin is rapidly targeted for degradation by the β-catenin destruction complex, unless the Wnt pathway has been activated.

As a signaling component, β-catenin is critically involved in the early development of the body axis through cellular polarity and anterior/posterior determination in both animals and humans (Haegel, 1995; Eberhart, 2001; Petersen and Reddien, 2009). In Wnt/β-catenin signaling, β-catenin can bind to the TCF/LEF family (TCF1, TCF3, TCF4, LEF1) of transcription factors, subsequently binding to promotor regions of genes such as CyclinD1 (Tetsu, 1999; Shutman, 1999), Myc (He, 1998), c-Jun (Mann, 1999). B-catenin must bind to these partners since it does not have a DNA binding domain of its own (Huber, 1997; Xing, 2008), acting as a transcriptional activator rather than directly as a transcription factor. Additionally, without β-

catenin, the TCF proteins actually become transcriptional repressors through binding to a Groucho/TLE repressor complex. When β-catenin binds, it displaces Groucho/TLE, turning off the repressor function of the TCFs and turning on their transcriptional activation, allowing for expression of Wnt response elements (WREs) and Wnt target genes (Daniels, 2005; Arce, 2009).

β-catenin can also bind to other transcription factors not directly involved in Wnt signaling, for example the HIF-1α target genes (Kaidi, 2007; Mazumdar, 2010) in hypoxic conditions, eventually causing a downstream decrease in TCF/β-catenin targeted transcription. Furthermore, the hypoxic conditions trigger the expression of the transcription factor FOXO, another potential binding partner for β-catenin, which subsequently increases its transcriptional activation (Essers, 2005). B-catenin has also been found to bind to Sox17 (Sinner, 2004; Archbold, 2012) during gastrulation, and even Oct4 (Kelly, 2011). B-catenin has also been shown to be involved in chromatin remodeling through promoting acetylation (Sekiya, 2007; Wray, 2011), and ubiquitination and trimethylation of histones (Sierra, 2006).

As a truly multifunctional protein with a multitude of pathways and partners it can interact with, β-catenin is a critically important molecule in the cell. Its potential dysregulation could interrupt any or all of its factors discussed above and is the reason why its study in disease is so lucrative yet challenging.

1.6 Wnt/β-catenin signaling in the heart

In cardiac development, Wnt/β-catenin signaling is critical for early embryonic cardiac development (Gessert, 2010) and the differentiation of embryonic stem cells into subtypes of myocytes (Liang, 2020), but the Wnt/β-catenin signaling pathway is quiescent in the healthy adult heart. However, β-catenin in the adult heart can be found as part of the cadherin complex, a

type of adherens junction. The typical cadherin complex in the heart is formed with N-cadherin at the intercalated disks, aiding in the mechanical and electrical coupling between adjacent cardiomyocytes. Phosphorylation of β-catenin's serine residues uncouples the cadherin complex, allowing for a switch so β-catenin may perform its role in mediating Wnt signaling (Piedra, 2003; Brembeck, 2004).

The role of Wnt/β-catenin signaling in heart disease has been studied, but with no overall consensus being achieved. There are multiple reports which suggest that activation of Wnt/β-catenin signaling in post-MI murine hearts was beneficial and cardioprotective, attenuating the loss of heart function. One study reported that post-MI rats treated with viral overexpression of constitutively active β-catenin in the infarct's border zone had reduced infarct sizes, as well as reduced apoptosis, increased capillary density, and cell cycle activity indicative of cellular proliferation (Hahn 2006). Two knockout mouse studies also reported that inhibition of the canonical Wnt/β-catenin pathway improved heart function post MI. With ablation of *Lrp5*, coding for one of the co-receptors for canonical Wnt signaling, the post-MI mice had a much greater infarct area than their wild-type littermates, indicating a protective effect for Lrp5/Wnt signaling in these mice (Borrell-Pages, 2016). A fibroblast-specific β-catenin deletion mouse line showed that ischemia/reperfusion (I/R) injury was exacerbated in knockout mice, suggesting that the Wnt/β-catenin activation in cardiac injury plays a critical role in cardiac function preservation (Duan, 2012).

However, other studies have also reported that activation of Wnt/β-catenin signaling appears to exacerbate post-MI outcomes, and that inhibition of these pathways improves cardiac outcomes. Mice overexpressing sFRP-1 (Wnt inhibitor) under the cytomegalovirus promotor displayed reduced cardiac dysfunction and occurrence of cardiac rupture post-MI, attributable to

decreased infarct apoptosis, decreased fibrosis, and increased angiogenesis (Barandon, 2003). Wnt3a protein injection in post-MI mouse myocardium resulted in decreased regeneration, wall thickness, and cardiac function, suggesting activation of Wnt signaling further decreased post-MI structural and functional remodeling (Oikonomopoulos, 2011). In addition, cardiomyocyte-specific β-catenin knockout mice had attenuated cardiac dysfunction, scar size, and hypertrophy by 4 weeks post-MI, as compared to wild-type controls. Furthermore, the improved cardiac function phenotype in β-catenin knockout mice was not attributable to reduced cellular hypertrophy or apoptosis but could be linked to increased resident cardiac progenitor cell population and differentiation within the infarct zone (Zelarayan, 2008).

Previous work from our lab has demonstrated that increased Wnt/β-catenin signaling, via adenoviral overexpression of Wnt3a in adult rat hearts, reduced cardiac Na^+ channel ($Na_v1.5$) expression (Lu, 2020). In addition, this was associated with an increased susceptibility to ventricular arrhythmias. Additionally, previous studies have used β-catenin gain-of-function (GOF) mouse models where exon 3 (encoding for the phosphorylation sites targeted by GSK-3β) is deleted, resulting in mutant β-catenin which is resistant to degradation, which allowed for greatly increased signaling pathway transduction. These β-catenin GOF mice also had reduced $Na_v1.5$ expression and sodium current (Huo, 2019). Others have also shown that Wnt/β-catenin signaling activation inhibits cardiac Scn5a expression in a dose and time dependent manner in a mouse atrial myocyte cell line (Wang 2016). In combining the findings from post-MI Wnt modulation studies and the effects of Wnt signaling overexpression and inhibition on cardiac ion channels, the evidence points to a potential link between Wnt signaling in heart disease and arrhythmias due to ion channel dysregulation. The critical role of the cardiac sodium channel in maintaining regular action potential morphology may be seriously implicated if the Wnt

signaling response somehow alters or affects sodium current, especially in the vulnerable post-MI heart.

2. Objectives and Hypotheses

Objective 1. To determine if ventricular arrhythmias are affected by inhibition of β-catenin after myocardial infarction.

Hypothesis: Inhibition of Wnt signaling, using β-catenin knockout mice in which cardiomyocytes are non-responsive to Wnt stimulation, protects the heart from ventricular arrhythmias.

Objective 2. To determine which Wnt pathway genes are upregulated in cardiomyocytes after myocardial infarction (MI), and if ion channel alterations after MI are affected by β-catenin deletion.

Hypothesis: Wnt signaling is activated in the myocardium after MI, and β-catenin deletion attenuates ion channel alterations.

3. Manuscript Text - Methods, Results and Discussion

(Accepted for publication in *Scientific Reports*)

Cardiomyocyte-specific deletion of β-catenin protects mouse hearts from ventricular arrhythmias after myocardial infarction

Jerry Wang[1,2], Ying Xia[1,2], Aizhu Lu[1,2], Hongwei Wang[1],

Darryl R. Davis[1,2], Peter Liu[1,2], Rob S. Beanlands[1] and Wenbin Liang[1,2,*]

[1] University of Ottawa Heart Institute,

[2] Department of Cellular and Molecular Medicine, University of Ottawa, Ottawa, ON, Canada

Short Title: β-catenin inhibition reduces ventricular arrhythmias

*Corresponding author:

Wenbin Liang, MD, Ph.D

Cardiac Electrophysiology Laboratory

University of Ottawa Heart Institute

Ottawa, ON, K1Y 4W7, Canada

Abstract

Wnt/β-catenin signaling is activated in the heart after myocardial infarction (MI). This study aims to investigate if β-catenin deletion affects post-MI ion channel gene alterations and ventricular tachycardias (VT). MI was induced by permanent ligation of left anterior descending artery in wild-type (WT) and cardiomyocyte-specific β-catenin knockout (KO) mice. KO mice showed reduced susceptibility to VT (18% vs. 77% in WT) at 8 weeks after MI, associated with reduced scar size and attenuated chamber dilation. qPCR analyses of both myocardial tissues and purified cardiomyocytes demonstrated upregulation of Wnt pathway genes in border and infarct regions after MI, including Wnt ligands (such as *Wnt4*) and receptors (such as *Fzd1* and *Fzd2*). At 1 week after MI, cardiac sodium channel gene (*Scn5a)* transcript was reduced in WT but not in KO hearts, consistent with previous studies showing *Scn5a* inhibition by Wnt/β-catenin signaling. At 8 weeks after MI when Wnt genes have declined, *Scn5a* returned to near sham levels and K^+ channel gene downregulations were not different between WT and KO mice. This study demonstrated that VT susceptibility in the chronic phase after MI is reduced in mice with cardiomyocyte-specific β-catenin deletion primarily through attenuated structural remodeling, but not ion channel gene alterations.

Key Words: Ventricular arrhythmia, Myocardial infarction, Heart failure, Wnt signaling, β-catenin

Introduction

Each year, ventricular tachyarrhythmia-induced sudden cardiac death (SCD) claims the lives of millions of people worldwide, including ~370,000 Americans[1] and ~700,000 European people.[2] Ischemic heart disease- (myocardial infarction, MI) is the most common underlying disorder and accounts for 65-80% of the SCD cases[3]. In post-MI hearts, ventricular tachyarrhythmias (including tachycardia and fibrillation, VT/VF)[4,5] result from both structural remodeling of the injured heart, i.e. fibrosis and scar formation in the infarcted region, and alterations in expression of ion channels/transporters especially in the border zone of the infarct,[6-8] such as reduced Nav1.5[9] and Cx43[10] as well as re-distribution of Cx43 (less in intercalated disk, but more in lateral surface of myocytes)[10]. The scar tissues are often interspersed with bundles of live cardiomyocytes, which form "re-entry circuits" together with border zone myocardium that have reduced and heterogenous conduction velocity, providing the substrate for VT/VF[6]. The alterations in ion channels in survived myocardium also increases their automaticity or triggered activity[11] that can initiate VT/VF.

Wnt signaling is critical for embryonic cardiogenesis[12] and we have recently shown that it regulates the differentiation of embryonic stem cells into different subtypes of cardiomyocytes.[13] In the canonical Wnt/β-catenin pathway, the binding of Wnt ligands to their plasma membrane receptors leads to the cytoplasmic accumulation of β-catenin, followed by its translocation into the nucleus and activation or inhibition of the transcription of target genes. In healthy adult hearts, Wnt/β-catenin signaling has a low activity but recent studies have suggested that its activity is increased in the myocardium in both human ischemic heart failure[14] and animal models of myocardial infarction[15] and heart failure,[16] as well as in murine models of pressure cardiac hypertrophy induced by pressure overload or angiotensin II.[17-20] However, one study reported that

increased Wnt/β-catenin signaling was only found in the myocardium of post-MI pigs with hypercholesterolemia, but not in post-MI pigs with normal cholesterol levels.[18]

Recent studies, including those from our group,[22-24] have demonstrated the capability of Wnt/β-catenin signaling to regulate the expression of cardiac sodium channel gene *Scn5a* (encoding $Na_v1.5$)[22-28] However, it remains unknown if Wnt/β-catenin signaling plays a role in the post-MI alterations in cardiac ion channel genes.

On the other hand, previous studies have not reached a consensus regarding the role of Wnt/β-catenin signaling in the structural remodeling of post-MI hearts. Several studies have suggested that Wnt/β-catenin signaling is cardioprotective and reduces scar size. In post-MI rats, viral expression of a constitutively active form of β-catenin in the border zone reduced infarct size, which is associated with reduced apoptosis and increased cell proliferation in both cardiomyocytes and fibroblasts.[29] In mice with deletion of Lrp5, the co-receptor required for Wnt/β-catenin pathway activation, the infarct size after MI was larger than in wild-type mice.[21] In mice with fibroblast-specific deletion of β-catenin, ischemia/reperfusion injury induced accelerated LV dilation and pump dysfunction.[15] By contrast, other studies have suggested a detrimental role of Wnt/β-catenin signaling. In post-MI mice, enhancement of the Wnt/β-catenin signaling in myocardium via Wnt3a protein injection accentuated cardiac dysfunction by inhibition of cardiac progenitor cell proliferation and endogenous regeneration.[30] Mice overexpressing FrzA (Sfrp-1), an inhibitor of Wnt signaling, had reduced scar size and cardiac rupture after MI, which are associated with reduced cell apoptosis in the scar region.[31] In mice with αMHC-Cre mediated β-catenin deletion, which made the cells non-responsive to Wnt stimulation, the scar size after MI was smaller which was associated with enhanced differentiation of a cardiac progenitor population

(marked as αMHC+/TAGA4+/Tbx5+, but cTnT-) into small cTnT+ cardiomyocytes in the infarcted region.[32]

In the present study we demonstrated for the first time that mice with cardiomyocyte-specific deletion of β-catenin have reduced susceptibility to ventricular tachyarrhythmias at 8 weeks after MI, which is associated with attenuated structural remodeling.

Methods

All procedures were approved by the institutional animal care committee at the University of Ottawa (Protocol #: HI-2602) and were performed in accordance with relevant guidelines and regulations. All the studies involving live animals were reported as described by the ARRIVE guidelines.[44]

Mice

To generate cardiomyocyte-specific β-catenin (*Ctnnb1*) knockout mice, *Ctnnb1*$^{flox/flox}$ mice (with exons 2 to 6 floxed, Jackson Lab, Stock No: 004152) were crossbred with αMHC-MerCreMer mice (Jackson Lab, Stock No: 005650) to obtain *Ctnnb1*$^{flox/flox}$;αMHC-MerCreMer$^{+/-}$ mice (Figure 1A). Littermate *Ctnnb1*$^{flox/flox}$;αMHC-MerCreMer$^{-/-}$ mice were used as control wild-type mice. At the age of 8-12 weeks, all mice received daily subcutaneous injection of tamoxifen (20 mg/kg, [Sigma, Catalogue No.:T5648], dissolved in sunflower seed oil at 10 mg/ml) for 5 consecutive days (Figure 1B). At 7 days after the last tamoxifen injection, baseline surface ECG and echocardiogram were recorded before the experimental myocardial infarction surgery as described below. Both male and female mice were used to investigate any sex-specific effects. A

total of 55 male mice (28 WT and 27 KO) and 72 female mice (38 WT and 34 KO) were used in this study.

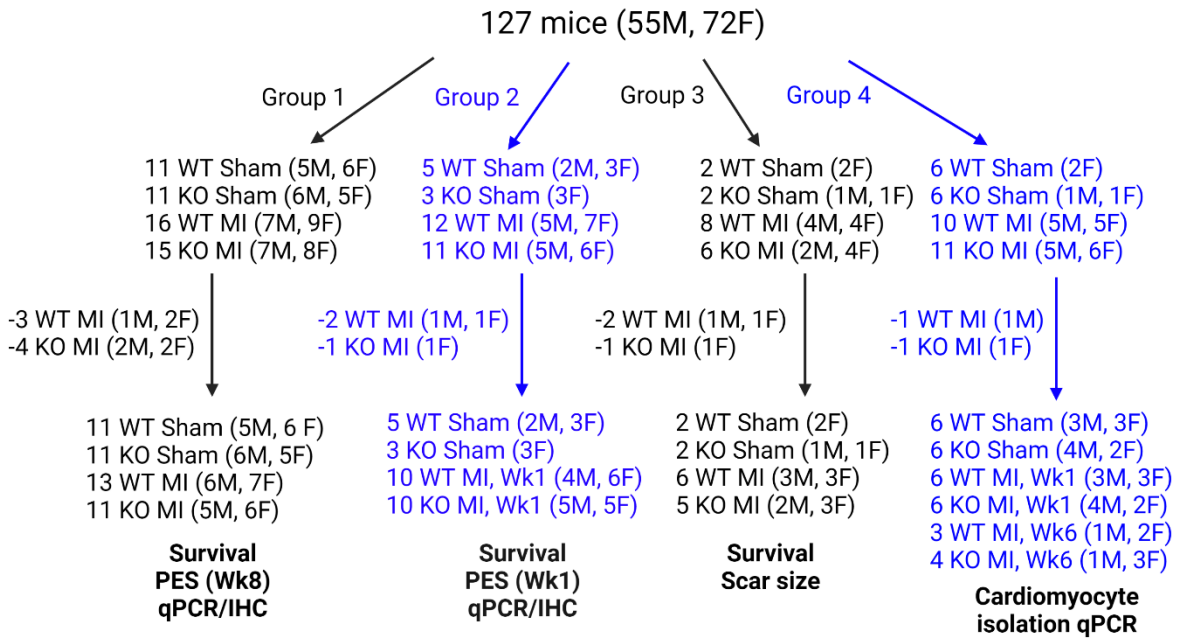

Figure iv. Mouse randomization, endpoint experiment, and sample post-processing.

Experimental Myocardial Infarction

Myocardial infarction was induced in mice by permanent ligation of the left coronary artery (LCA) as we previously described.[53] Mice were injected with buprenorphine (0.05 mg/kg; subcutaneous) 1 hour prior to surgery and twice daily thereafter for 3 days. During the surgery, mice were intubated, anesthetized using 2% isoflurane, and maintained under physiologic temperature control. After exposing the heart via left thoracotomy, the LCA was identified under a dissection microscope (Topcon Corporation, Model No.: OMS-75) and ligated at 0.3 mm distal to the atrioventricular junction using a Prolene 7.0 suture. Successful LCA ligation was confirmed during the surgical procedure by the pale color of the affected myocardium before chest closure with a Prolene 6.0 suture. At the week 1 timepoint, successful MI surgery was

confirmed by a reduction of ≥20% EF compared to baseline heart function. Any animals whose ΔEF% was <20% was excluded from further analysis and studies.

Surface ECG and Echocardiography

ECG with limb Lead I and II were recorded in mice at one day before and at week 1, 3, 5 and 8 after the LAD ligation using ADInstruments small animal ECG system (Powerlab 8/35 and Animal Bio Amp) and data were analyzed using LabChart 8.0. During ECG recording, mice were anesthetized with 1.5-2.0% isoflurane and body temperature was kept at 37°C using a heating pad. Mouse ECG parameters were analyzed in LabChart 8 software (version 8.1.5, ADInstruments) software. In brief, automated averaging of 10 consecutive beats was done by the software. Three consecutive "averaged cycles" were analyzed, and these values were finally averaged. To manually correct the auto-detected intervals if they were incorrectly placed: the PR interval was measured from onset of the P wave to the onset of the QRS complex (in cases where the Q wave was not very visible, the onset of the R wave was used). The QRS duration was measured from onset of the QRS complex to the return to baseline voltage following the S wave (or if there was no return to baseline, the peak positive deflection following the S wave was used). The QT interval was measured from onset of the QRS complex to the return to baseline voltage following the T wave.

Echocardiography

Echocardiography was recorded using a VEVO3100 system with the MS400 transducer (VisualSonic Inc., Toronto), and images were analyzed in VevoLab software. During recording, animals were anaesthetized under 1.5-2% isoflurane with body temperature maintained at 37°C

using a heating pad. To minimize the influence of heart rate on pump function, echocardiogram was recorded when heart rates were in the 400-500 bpm range. M-mode tracing of the left ventricle (LV) was recorded in the short-axis view at the mid-papillary level. Three consecutive cardiac cycles, measured in VevoLab, were averaged to determine ejection fraction % (EF), fractional shortening % (FS), end-diastolic volume (EDV), end-systolic volume (ESV), left ventricular internal diameter (LVIDs/LVIDd), and posterior wall thickness. The EF was calculated using the following equation: $(LVIDd^3–LVIDs\ d3^3)/LVIDd^3\times100$. FS was calculated using the following equation: (LVIDd–LVIDs)/LVIDd×100. B-mode tracing of the LV was recorded in the parasternal long-axis view and analyzed using the LV trace function in VevoLab to determine EF, FS, EDV, ESV, and LV volume. EF was used preferentially over FS in drawing our conclusions due to the regional wall motion abnormalities associated with MI, and the inability of FS to capture these differences.

Programmed electrical stimulation (PES) in isolated mouse hearts

At 1 and 8 weeks after MI, mouse hearts were isolated and Langendorff-perfused with Tyrode solution (37°C) containing 1 μM isoproterenol (Sigma, Catalogue No.: I6504), while *ex vivo* ECG was continuously measured by placing recording electrodes around the heart as we previously described[20,46] (Figure 1E). PES was applied using a MyoPacer (IonOptix) via a pair of platinum electrodes placed on the left ventricular apex of the heart. The standard stimulation protocol (Figure 1E) consisted of 10 stimuli at 100 ms intervals (S1, 5V) followed by one extra stimulus (S2) starting at an interval of 80 ms, which was then reduced by 2 ms until the effective refractory period (ERP) was reached. If VT or VF was not induced, a second extra stimulus (S3) was added at 80 ms after S2. The S3 interval was then reduced by 2 ms until the ERP was reached. Finally, a

third extra stimulus (S4) was added 80 ms after S3 and was then decreased by 2 ms until the ERP was reached. If a heart failed to develop a VT or VF with 3 extra stimuli, the heart was deemed non-inducible.

Masson's Trichrome staining

Mouse hearts were fixed by retrograde perfusion via the aorta with 4% paraformaldehyde (diluted in PBS) for 10 min at room temperature. The hearts were then incubated in increasing concentrations of sucrose dissolved in PBS (10% for overnight, 20% for 8 h, and 30% for overnight) on a horizontal rotator at 4°C before being embedded in TissueTek OCT compound. Hearts were then cryosectioned at 10-µm slices using a Leica vibrating microtome (Model No.: CM3050S) at five different levels of the heart from the ligation site to the apex at 300-µm intervals. Ten consecutive slices were made for each level. Heart sections were then stained using a Masson's Trichrome Staining kit (Sigma, Catalogue No.: HT15) according to the manufacturer's instructions. Fibrosis areas were analyzed with ImageJ software using the Colour Deconvolution for Masson's Trichrome Stain tool. The scar size for each the 5 different levels was calculated as the percentage of fibrotic area to the total area of the left ventricle section. The heart's total scar size was then calculated as the mean of the scar sizes at the 5 levels and reported in Figure 4.

Immunohistostaining

Cryosectioned heart slices, as prepared above, were blocked and permeabilized in Dako protein block (Agilent, Catalogue No.: X0909) containing 0.1% (w/v) saponin (Sigma, Catalogue No.: 47036) at room temperature for 90 min. Slices were incubated with primary antibodies (see

below) diluted in the same blocking solution at 4°C for overnight. After washing with PBS, slices were incubated with secondary antibodies (see below) at room temperature for 1 h. After washing with PBS three times, slices were mounted with ProLong gold antifade reagent containing DAPI (ThermoFisher, Catalogue No.: P36931). Primary antibodies used were polycloncal rabbit anti-Cx43 (1:200, Sigma, Catalogue No.: C6219) and monoclonal mouse anti-α-sarcomeric actinin (1:400, Sigma, Catalogue No.: A7811). Secondary antibodies used were anti-rabbit IgG (Alexa Fluor-488, 1:300) and anti-mouse IgG (Alexa Fluor-568, 1:300). Fluorescent images of the myocardium of left ventricular free wall of sham hearts and border zone of MI-hearts were taken with a ZEISS confocal microscope equipped with the Airyscan technique for high-resolution imaging (Zeiss Elyra S.1 LSM 880).

Isolation of single ventricular myocytes

Single ventricular myocytes were isolated from adult mouse hearts according to a protocol we previously described.[54-56] Mouse hearts were isolated and perfused on a Langendorff system with a nominally calcium-free Tyrode solution (in mmol/L: 136 NaCl, 5.4 KCl, 0.5 Na_2HPO_4,10 HEPES, 1 $MgCl_2$, and 10 glucose, pH=7.40 with NaOH) at 37°C for 10 min. Collagenase (1 mg/ml, type II, Worthington Biochemical Inc. Catalogue No.:LS004177) and protease (0.028 mg/ml, type XIV, Sigma, Catalogue No.: P5147) were added into the calcium-free Tyrode solution and the hearts were perfused for another 15-20 min. The left ventricular tissue containing the infarct and boarder zone (in MI hearts) or the left ventricular free wall (in sham-operated hearts) was dissected and cut into small pieces in KB solution (in mmol/L: 100 K-glutamate, 10 K-aspartate, 2.5 KCl, 10 KH_2PO_4, 2 $MgSO_4$, 5 HEPES, 20 glucose, 20 taurine, 5 creatine, 0.5 EGTA, and 0.1% albumin, pH=7.2 with NaOH). Single cardiomyocytes were

released in KB solution by gentle pipetting. Cell suspension was kept on ice and allowed to settle for 10 min. A small aliquot (50 μL) of the cells were stained with Hoechst 33342 (0.1 μg/ml, ThermoFisher, Catalogue No.: 62249) for 10 min and cell images were taken using a fluorescent microscope (Leica Microsystems, Model No.: DMi8) equipped with a DAPI filter cube and a 40x objective. Cardiomyocytes settled to the bottom, while other cell types (such as fibroblasts, vascular endothelial and smooth muscle cells, and immune cells) remained in the supernatant (Figure 7A). The cell pellet containing pure cardiomyocytes were used for RNA extraction and real-time PCR analysis.

Real-Time Quantitative PCR (qPCR)

Total RNA was isolated from the border zone and infarct region of mouse hearts with Trizol reagent (ThermoFisher, Catalogue No.: 15596026) and digested with Turbo DNA-*free* kit (ThermoFisher, Catalogue No.: AM1907) to remove genomic DNA, according to the manufacturer's instructions. Total RNA from purified ventricular myocytes was extracted using a RNeasy Micro kit (Qiagen, Catalogue No.:74004) and genomic DNA was removed by on-column digestion with RNase-Free DNase kit (Qiagen, Catalogue No.:79254) according to the manufacturer's instructions. One μg RNA was used for cDNA synthesis with a High-Capacity cDNA Reverse Transcription Kit (ThermoFisher, Catalogue No.: 4368814). Real-time quantitative PCR was performed on a CFX Connect Real-Time PCR Detection System (Bio-Rad) using standard SYBR green method. Information of the qPCR primers was included in Table 1 in the Online Supplement. No reverse transcriptase (RT-) controls and no template controls (NTC) were included for all the primers to make sure that there were no genomic DNA

contamination or primer dimer signals. Transcript level of target genes was normalized to the level of *Hprt1* mRNA in the same sample. Results were analyzed with the $2^{-\Delta\Delta C(t)}$ method.

Western Blotting

The border zone myocardium tissue of the post-LAD ligation hearts (week 1 and 8) or the left ventricular anterior free wall of sham-operated hearts were homogenized in T-PER Tissue Protein Extraction Reagent (ThermoFisher, 78510) containing Halt Protease Inhibitor Cocktail (ThermoFisher, 87786). Protein concentration was determined using Pierce Rapid Gold BCA Protein Assay Kit (ThermoFisher, A53226) and cell lysates (10 μg protein per lane) were run on a 4-12% SDS-polyacrylamide gel and transferred onto a PVDF membrane. The transferred membrane was incubated with a primary antibody (see below) overnight at 4°C, followed by a 2-h incubation with a peroxidase-conjugated secondary antibody (1:2000, Cell Signaling, #7074). Primary antibodies used were rabbit anti-non-phospho (active) β-catenin (Ser33/Ser37/Thr41) (1:1000, Cell signaling, #8814) and rabbit anti-total β-catenin (1:1000, Cell signaling, #8480). Immunoreactivity was detected by chemiluminescence (Pierce™ ECL Western Blotting Substrate, ThermoFisher, 32209). Equal protein loading of the gels was assessed by re-probing the membrane with rabbit anti-GAPDH antibody (1:2000, Cell Signaling, #2118). Band densities were quantified using the "Gel Analyzer Protocol" function of ImageJ (https://imagej.nih.gov/ij/docs/menus/analyze.html#gels) and presented as values after normalization to GAPDH in the same samples. All the original uncropped gel images are included in Supplementary Figure 1.

Statistical Analysis

Statistical analysis adhered to the Journal Guidelines. Analysis of primary outcomes was not blinded. Data are expressed as mean ± SEM with $p<0.05$ considered significant. Sample number indicates the number of biological replicates (each individual mouse is considered one sample). Initial sample size calculation was performed using $\alpha=0.05$ and $\beta=0.2$, estimating incidence of arrhythmia inducibility (dichotomous endpoint) at 75% for the WT group and 25% for the KO group (two independent sample study), for a total of n=14 per group. Differences between two means were evaluated by two-tailed Student's *t*-test. Differences among multiple means were assessed by one-way or two-way analysis of variance (ANOVA). When significance was detected by ANOVA, differences among individual means were evaluated *post hoc* by Bonferroni's test.

Results

β-catenin knockout reduces the susceptibility to ventricular tachycardias after myocardial infarction

Successful knockout of β-catenin after tamoxifen treatment was confirmed by western blot showing marked reductions of β-catenin protein in the left ventricle of *Ctnnb1*$^{flox/flox}$;αMHC-MerCreMer$^{+/-}$ (KO) mice as compared to *Ctnnb1*$^{flox/flox}$;αMHC-MerCreMer$^{-/-}$ (WT) mice (Figure 1C). Post-MI survival curve showed that there was no difference ($p=0.75$) in the death rate between WT and KO groups (Figure 1D) with all the death (15% for WT; 19% for KO) occurring within the first week in both groups. The absence of animal deaths in the late stage after MI suggests no lethal arrhythmias in these mice. This reflects a known limitation of studying arrhythmias in mice—the low rates of spontaneous arrhythmias due to their fast heart rate, short action potential duration and smaller heart size, as compared to human and large animal models (e.g., monkeys and pigs) of heart disease.

To investigate the susceptibility of mice to ventricular arrhythmias, we used a protocol that we recently developed for rodent hearts[23,33] that combined adrenergic stimulation (with isoproterenol) and progressive programmed electrical stimulation (PES) in isolated, Langendorff-perfused hearts (Figure 1E), while *ex vivo* ECG was recorded by placing electrodes around the heart. With this protocol, ventricular tachycardias (VT, defined as three or more consecutive ectopic ventricular beats) were successfully induced in 77% (10/13) post-MI WT mice at week 8, but in none (0/18) of the sham-operated WT mice (Figure 1F and 1G) validating our VT-inducing protocol. No difference was observed between male and female mice in VT inducibility (4/5 in male and 6/8 in female, $p=0.84$) or arrhythmia score (Figure 1G) (3.40±0.60 in male and 3.13±0.58 in female, $p=0.76$). In contrast, VT was induced in only 18% (2/11) of the post-MI KO mice at week 8 indicating reduced susceptibility to ventricular arrhythmias ($p<0.05$ vs. WT, Figure 1G). Interestingly, a significant portion of the KO mice at week 8 after MI (55% vs. 15% in WT) exhibited isolated or coupled PVCs that did not develop into VT even when stimulated with the maximum PES strength of 10x S1 (100ms) + S2 (80ms) + S3 (80ms) + S4 ((Figure 1G). At week 1 after MI when the scar tissue was still immature, the majority of WT and KO hearts only exhibited isolated or coupled PVCs with VT induced in only one WT heart (Figure 1G), suggesting a low inducibility of VT at this subacute phase.

β-catenin knockout reduces the prolongation of QRS duration and QT interval after myocardial infarction

Surface ECG recording in live animals showed no difference between sham-operated KO and WT mice in any of the parameters analyzed (QT interval, QRS duration, PR internal and RR internal, Figure 2). WT mice that received LAD ligation (MI) surgery exhibited prolonged QT interval

(starting at week 1) and increased QRS duration (starting at week 3), but showed no changes in PR or RR intervals, suggesting that MI led to left ventricular remodeling without significantly affecting the function of the central conduction system (sinoatrial node and atrioventricular node), although it is not clear if the intrinsic heart rate (i.e. after blocking the effects of autonomic nervous system) is altered. The MI-induced QT interval prolongation and QRS duration increases were attenuated in KO mice compared with WT mice (Figure 2), which is consistent with reduced VT susceptibility in KO mice.

β-catenin knockout attenuates chamber dilation and pump dysfunction after myocardial infarction

Echocardiography (Figure 3A) showed no difference between sham-operated KO and WT mice in LV chamber dimension (end diastolic volume, EDV, Figure 3B) or pump function (ejection fraction, EF, Figure 3C). Post-MI WT mice exhibited marked LV dilation (EDV=118.0±16.5 µl, n=14 vs. 42.0±2.5 µl, n=9 in sham WT at week 8, $p<0.01$, Figure 3B) and pump dysfunction (EF=21.6±3.3%, n=14 vs. 64.7±1.5%, n=9 in sham WT at week 8, $p<0.01$, Figure 3C), but LV posterior wall thickness (LVPWd) was not changed ($p=0.7488$ by ANOVA, Figure 3D). In post-MI KO mice, LV dilation (EDV=77.8±7.8µl, n=13 vs. 44.4±3.1 µl, n=10 in sham KO at 8-week, $p=0.064$, Figure 3B) and pump dysfunction (EF=34.9±4.3%, n=13 vs. 65.3±1.1%, n=10 in sham KO at 8-week, $p<0.01$, Figure 3C) were attenuated ($p<0.01$) compared with post-MI WT mice.

β-catenin knockout reduces scar sizes after myocardial infarction

Masson's trichrome staining of sham-operated hearts did not show any difference in gross morphology between KO and WT mice (Figure 4A). Consistent with observations in

echocardiogram, post-MI WT hearts showed LV chamber dilation and wall thinning (Figure 4A). The scar size, as determined by the % fibrotic area of the LV wall, was smaller in post-MI KO (Scar size 38.5±3.9%, n=5 vs. 50.3±3.1%, n=6 in post-MI WT at 8-week, $p<0.05$, Figure 4B).

Upregulation of Wnt pathway genes in myocardium after myocardial infarction

Wnt pathways are fine-tuned by the soluble Wnt ligands and Wnt inhibitors on the extracellular side of the plasma membrane, as well as the receptors and co-receptors on the plasma membrane (Fig. 5A). Our qPCR analyses of gene transcripts of the myocardial tissues, which contained both cardiomyocytes and other cell types such as fibroblasts (Fig. 5B), showed that a variety of Wnt ligands, inhibitors and receptors are upregulated in the border zone and infarct region of the mouse hearts after MI (Fig. 5 and 6).

Wnt ligands (Fig. 5C): *Wnt1*, a canonical Wnt ligand known to selectively activate the β-catenin pathway, was increased by 3-7 fold after MI ($p<0.05$ in WT infarct at week 1 vs. WT sham; $p<0.05$ in KO infarct at week 8 vs. KO sham) and *Wnt3a*, another canonical Wnt ligand, was increased by ~2 fold ($p<0.05$ in WT border at week 1 vs. WT sham). *Wnt7*, a noncanonical Wnt ligand that selectively activate the β-catenin-independent pathways, was increased by ~20 fold in the infarct ($p<0.05$ in WT infarct at both week 1 and 8 and border at week 8 vs. WT sham, $p<0.05$ in KO infarct vs. KO sham). Six Wnt ligands (*Wnt4, Wnt10a, Wnt2, Wnt5b, Wnt6 and Wnt9a*) that have been reported to activate both β-catenin dependent and independent pathways or have less defined functions, were also increased after MI: *Wnt4* was increased by ~30 fold in infarct at week 1 ($p<0.01$ in KO infarct vs. KO sham), *Wnt10* increased by ~5 fold in infarct ($p<0.05$ in KO infarct at week 1 and 8 vs. KO sham), *Wnt2* showed a trend of increase in infarct at week 8 ($p<0.05$ in KO infarct vs. KO sham), *Wnt5b* was increased by 2-3 fold ($p<0.01$ in WT border and infarct at

week 1, and $p<0.05$ in WT infarct at week 8 vs. WT sham), *Wnt6* was increased by 49% in KO infarct at week 8 ($p<0.05$ vs. KO sham), and *Wnt9a* was increased by 92% in KO infarct at week 8 ($p<0.05$ vs. KO sham).

Wnt inhibitors (Fig. 5D): Secreted frizzled-related proteins (Sfrp) are soluble Wnt inhibitors that prevent the binding between Wnt ligands and their plasma membrane receptors (frizzled).34 At week 1 after MI, *Sfrp2* showed the largest increase in both border and infarct (by 97-256 fold, $p<0.05$ vs. WT sham or KO sham), *Sfrp3* also showed significant increases (by 16-32 fold, $p<0.05$ vs. WT sham or KO sham) and *Sfrp1* was increased by ~30 fold in the infarct ($p<0.05$ vs. WT sham or KO sham). At week 8, all three *Sfrp* levels have declined in border zone but remained high in the infarct region ($p<0.05$ vs. WT sham or KO sham). Dickkopf-related proteins (Dkk) are another group of soluble Wnt inhibitors that selectively inhibit Wnt/β-catenin pathway by causing endocytosis of Wnt co-receptors (Lrp5/6) from the plasma membrane.35 *Dkk3* was increased by 6-11 fold at week 1 ($p<0.05$ vs. WT sham or KO sham) and was further increased to 22-32 fold in the infarct at week 8 ($p<0.05$ vs. WT sham or KO sham). *Dkk1* was marginally increased by 1.3-2.0 fold ($p<0.05$ in KO border at week 1 vs. KO sham, $p<0.05$ in WT infarct at week 8 vs. WT sham), while *Dkk4* was not affected by MI ($p=0.801$).

Wnt receptors and co-receptors (Fig. 6): Frizzled (Fzd) proteins are seven-transmembrane proteins that serve at the receptors for Wnt ligands on the plasma membrane (Fig. 5A). Among the 9 *Fzd* genes, the mostly affected by MI were *Fzd1*, *Fzd2* and *Fzd5* that were increased in border and infarct at week1 by 5-7 fold ($p<0.05$ vs. shams), 8-13 fold ($p<0.05$ vs. shams) and 2-4 fold ($p<0.05$ vs. shams), respectively. But in the border zones at week 8 they all showed a significant decline. *Fzd7*, *Fzd8* and *Fzd3* in infarct were increased at week 1 ($p<0.05$ vs. shams), and *Fzd7* and *Fzd8* in infarct remained high at week 8 ($p<0.05$ vs. shams). *Fzd9* showed no changes at week 1 but was

increased at week 8 in infarct ($p<0.05$ in WT infarct vs. WT sham). The other two *Fzd* genes in the family (*Fzd4* and *Fzd6*) were not changed after MI ($p>0.20$ and $p>0.22$, respectively). Lipoprotein receptor-related protein 5 and 6 (Lrp5/6) are co-receptors required for Wnt ligand-induced activation of β-catenin pathway (Fig. 5A). *Lrp5* showed a 1.7-2.3 fold increase at week 1 ($p<0.05$ in WT infarct and in KO border vs. shams). *Lrp6* also showed a 1.7-2.3 fold increase at week 1 ($p<0.05$ in WT infarct and in KO border vs. shams), and a ~2 fold increase in infarct at week 8 ($p<0.05$ in KO infarct vs. KO sham). But in the border zone at week 8 both *Lrp5* and *Lrp6* returned to near sham levels. *Ror2* and *Vangl2* are co-receptors required for non-canonical Wnt mediated activation of β-catenin-independent pathways. *Ror2* and *Vangl2* were increased in both border and infarct at week 1 by 4-9 fold and 2-4 fold ($p<0.05$ vs. WT or KO shams), respectively, and they also showed a significant decline in border zone at week 8.

β-catenin protein: In cells not stimulated with Wnt/β-catenin pathway ligands, β-catenin in the cytoplasm is phosphorylated at Ser33/Ser37/Thr41 which labells them for ubiquitination and degradation.36 The level of β-catenin that is not phosphorylated at Ser33/Ser37/Thr41 (i.e., active β-catenin) is an index of the Wnt/β-catenin pathway activation in the cells.37 As shown in Fig. 6C, active β-catenin was increased by 4.9 fold in the border zone myocardium of WT hearts at 1 week after LAD ligation ($p<0.01$ vs. WT sham), suggesting activation of the Wnt/β-catenin pathway in the myocardial tissue. An increase in active β-catenin at 1 week (3.9 fold, $p<0.05$) was found in KO hearts in which only the cardiomyocytes were deleted of β-catenin. This suggests activation of the Wnt/β-catenin pathway at 1 week in non-cardiomyocytes (such as fibroblasts and inflammatory cells). In addition, the increased total β-catenin in KO hearts at 1 week also suggests an increased proportion of non-cardiomyocytes (e.g., by fibroblast proliferation and infiltration of inflammatory cells) in the border zone myocardium.

Upregulation of Wnt pathway genes in ventricular myocytes after myocardial infarction

In order to investigate if Wnt pathway genes are altered in cardiomyocytes after MI, single cardiomyocytes were isolated from the infarct and border tissues (or from the left ventricular free wall in sham-operated groups) after collagenase digestion of the hearts (Fig. 7A). Cardiomyocytes were purified by removing non-cardiomyocyte cells after settlement for 10 min (Fig. 7A). qPCR analysis of pure cardiomyocytes showed that many of the Wnt pathway genes are also upregulated after MI (Fig. 7B to 7D).

Wnt ligands (Fig. 7B): *Wnt4* was increased in cardiomyocytes by 17-38 fold at week 1 ($p<0.05$ in KO vs. sham), which is similar to its increase in myocardial tissue (~30 fold). *Wnt10* showed a trend of 8-13 fold increase in cardiomyocytes at week 1($p=0.06$ in KO vs. sham). *Wnt2* showed a trend of 4-6 fold increase in cardiomyocytes at week 1 ($p=0.06$ in both WT and KO vs. shams). *Wnt1* was increased but to a lesser degree (by ~30%, $p<0.05$) than in myocardial tissue (by 3-7 fold), while Wnt3a was not affected in cardiomyocytes ($p>0.25$) after MI. *Wnt7* was increased by 6-13 fold ($p<0.05$, WT week 1 vs. WT sham), which is less than its increase in myocardial tissue (20 fold).

Wnt inhibitors (Fig. 7C): *Sfrp2* was increased by 52-68 fold in cardiomyocytes at week 1 ($p<0.05$ in KO vs. sham) and by 16 fold at week 6 ($p<0.05$ in KO vs. sham), which were less than its increase in myocardial tissues (97-256 fold at week 1). *Sfrp1* and *Sfrp3*, which had ~30 fold increases in myocardial tissues at week 1, were increased in cardiomyocytes by 8-17 fold and 8-12 fold, respectively ($p<0.05$ in both WT and KO vs. shams) but were not significantly affected at week 6. *Dkk3* was increased by 7-13 fold at week 1 ($p<0.05$ in both WT and KO vs. sham) which

is similar to its increase in myocardial tissues (6-11 fold), while *Dkk1* was not statistically affected ($p>0.09$) after MI.

Wnt receptors and co-receptors (Fig. 7D): *Fzd2*, which was increased by 8-13 fold in myocardial tissues at week 1, was increased in cardiomyocytes by 4-5 fold at week 1 ($p<0.05$ in both WT and KO vs. shams). Similarly, *Fzd1*, which was increased by 5-7 fold in myocardial tissue, was increased in cardiomyocytes by 2-3 fold at week 1 ($p<0.05$ in KO vs. sham). *Fzd7* was increased by 90% in KO at week 1 ($p<0.05$ vs. sham). *Fzd3*, *Fzd8* and *Fzd9* were not statistically affected by MI ($p>0.57$, $p>0.09$ and $p>0.33$, respectively). *Fzd5* was reduced by 40% in WT at week 1 ($p<0.01$ vs. WT sham) and reduced by 54% in KO at week 6 ($p<0.05$ vs. KO sham). *Lrp5* showed a trend of increase in cardiomyocytes at week 1 but was not statistically significant ($p=0.08$ in KO vs. sham), while *Lrp6*, which had a ~2 fold increase in myocardial tissue, was reduced in cardiomyocytes by 45% at week 1 ($p>0.05$ in WT vs. sham). *Ror2* was increased (by 5-8 fold, $p<0.01$) to a similar level in myocardial tissue (4-9 fold) at week 1. *Vangl2*, which was increased by 2-4 fold in myocardial tissue, was increased in cardiomyocytes only by 54% in KO at week 1 ($p<0.05$ vs. KO sham).

Ion channel gene expressions after myocardial infarction

Ion channels genes for ventricular depolarizing currents (Fig. 8A): In the border zone at week 1, the cardiac Na+ channel gene transcript (Scn5a, encoding Nav1.5) was reduced in WT hearts (0.544 ± 0.07, $n=7$ vs. WT sham 1.0 ± 0.07, $n=8$, $p<0.01$), but it was not reduced in β-catenin KO hearts (0.76 ± 0.15, $n=5$ vs. KO sham 0.90 ± 0.04, $n=9$, $p>0.99$). Because it is known that Wnt/β-catenin signaling reduces Scn5a level in cardiomyocytes,[22,23,25] these observations suggest that the Wnt/β-catenin pathway likely plays a role in Scn5a downregulation in the border zone of post-MI

hearts. In addition, the returning of Scn5a level to near sham level in WT border at week 8 (0.82±0.05, n=5 vs. sham 1.0±0.07, n=8, p=0.38) also mirrored the reduced Wnt signaling at this time point. The significant reductions of Scn5a transcript in the infarct tissue at both week 1 and 8 are likely a result of the increased proportion of non-cardiomyocytes in this tissue. The L-type Ca2+ channel gene (Cacna1c, encoding Cav1.2) was increased by 3.3 fold ($p<0.05$) in both border and infarct tissues at week 1 as compared to sham groups. However, at week 8 Cacna1c in the border zone has returned to near sham levels. The high level of Cacna1c in infarct may reflect the expression of this channel in fibroblasts38 which are abundant in infarct tissues.

Ion channels genes for ventricular repolarizing currents (Fig. 8A): All the major ventricular K^+ channel genes, including I_{to} (*Kcnd2, Kcnd3*), I_{Kr} (*Kcnh2*), I_{Ks} (*Kcnq1*) and I_{K1}(*Kcnj2*), were reduced ($p<0.05$) in border and infarct tissues at both week 1 and 8 as compared to sham groups. Consistent with our previous findings that Wnt signaling does not affect I_{K1} or action potential repolarization[22], no differences were seen between KO and WT groups in these K^+ channel genes after MI.

<u>*Gap junctions and HCN channels*</u>: In the border zone, transcript of Cx43 (*Gja1*), the predominant gap junction isoform in ventricular myocardium, was reduced at week 1 but it returned to near sham levels at week 8 (Figure 8B). However, immunostaining of Cx43 protein in border zones of both KO and WT hearts at week 8 showed that Cx43 is more diffusively distributed and is no longer restricted to cell-cell junction regions (intercalated disks) as seen in sham groups (Figure 7C). Cx40 (*Gja5*), which is expressed in the Purkinje fibers, was not affected by MI (Figure 7B). Among the genes of HCN channels that, if increased, will enhance myocyte automaticity, *Hcn1* was increased while *Hcn2* and *Hcn4* were reduced at week 1 but they returned to near sham levels

at week 8 (Figure 7B). Again, no differences were seen between KO and WT hearts in these gene transcript levels.

Discussion

Although Wnt/β-catenin signaling has been studied in animal models of ischemic heart disease, this is the first study to investigate the post-MI arrhythmogenesis using β-catenin knockout mice. The reduced susceptibility to VT in β-catenin KO mice after MI is likely due to attenuated structural remodeling. The low VT inducibility at week-1 in both WT and KO mice when the scar was immature and at week-8 in KO mice that had a smaller scar highlights the importance of structural remodeling in VT induction. Previous studies in patients have also demonstrated a positive relationship between scar sizes and the risk for VT.[39] In addition, large scar sizes are associated with a longer cycle length for monomorphic VT,[40] further supporting the reentry as the predominant mechanism for VT in post-MI hearts.[41]

The increased QRS duration, reflecting electrical dyssynchrony, is commonly found in heart failure patients and has been demonstrated to be an independent predictor of mortality in these patients.[42,43] Consistent with this, in the present study the increased QRS in post-MI WT hearts is associated with a greater VT inducibility. The increased QRS in these mice is likely secondary to the structural remodeling (scar and chamber dilation), as well as possible reductions in the conduction velocity of Purkinje fibers (arborization block) which is common in ischemic heart failure.[44] The QT interval and its dispersion are positively associated with the scar size in patients with MI and their increases are a risk factor for VT.[45] The attenuated increases in both QRS duration and QT intervals in β-catenin KO mice are consistent with their reduced VT inducibility and a smaller scar size.

The upregulation of Wnt pathway genes (such as *Wnt1* and *Wnt4*) in the myocardial tissue of post-MI hearts is consistent with previous studies.[15,16,46] In addition, the present study provided direct evidence for the upregulation of Wnt genes in cardiomyocytes. The similar levels of *Wnt4* increase (~30 fold) in myocardial tissues and purified cardiomyocytes suggest that it is upregulated at the same degree in both cardiomyocytes and other cell types (such as fibroblasts, vascular cells, and inflammatory cells). In contrast, other Wnt genes that are significantly increased in myocardial tissues are either upregulated at a lower level (such as *Wnt1* and *Wnt7*) or not increased (such as *Wnt3a*) in cardiomyocytes, suggesting differential levels of upregulation in these Wnt genes between cardiomyocytes and other cell types. This finding may be helpful for future designing of therapeutic strategies for cell type-specific interventions of the Wnt pathways in ischemic heart disease.

While previous studies have reported conflicting results regarding the role of β-catenin in post-MI structural remodeling, our observations that β-catenin KO mice had attenuated structural remodeling after MI are consistent with the study by Zelarayan *et al.*, which also found a smaller scar size in β-catenin KO mice at 4 weeks after MI (LAD ligation).[32] The study by Zelarayan *et al.* also suggested that enhanced cardiac regeneration via activation of a cardiac progenitor population in the infarcted region may be a mechanism for the reduced scar in β-catenin KO hearts.[32] However, future studies are needed to investigate if other mechanisms, such as reduced cardiomyocyte deaths (in the form of necrosis, apoptosis, necroptosis and pyroptosis) or enhanced cardiomyocyte survival, are also involved. In addition to its role as the intracellular mediator of the Wnt/β-catenin signaling, β-catenin is also expressed in the cytoplasmic side of the plasma membrane in the cell-cell junction region, where it interacts with other membrane proteins such as N-cadherin.[47,48] Future studies are needed to investigate if the deletion of β-catenin in

cardiomyocytes alters cell-cell interactions[46] within the ischemic myocardium as a potential mechanism for the attenuated post-MI structural remodeling.

The reduced *Scn5a* transcript level in WT hearts, but not in KO hearts, at 1 week after MI is consistent with previous observations by us and others that Wnt/β-catenin signaling reduces *Scn5a* levels in cardiomyocytes.[22-28] Our finding that *Scn5a* transcript returned to near sham levels in WT hearts at 8 weeks after MI is also consistent with the reduced Wnt gene levels at this timepoint as compared to 1 week. In addition, the similar levels of K^+ channel gene downregulations in both WT and KO hearts are consistent with our previous observation that Wnt/β-catenin signaling does not affect the resting membrane potential or the repolarization phase of action potentials in rat cardiomyocytes.[22] HCN channels have been shown to play a role in the arrhythmogenesis of dilated cardiomyopathy, and HCN2-overexpressing hearts have increased VT susceptibility.[49] In the present study, the selective upregulation of *Hcn1* gene is consistent with previous studies using a mouse model of cardiac hypertrophy, although *Hcn2* and *Hcn4* are more abundant than *Hcn1*.[50] One limitation of the present study is that ion channel genes were not analyzed on purified cardiomyocytes and fibroblasts. Of note, the cardiac fibroblasts are known to express voltage-gated K^+ channels and transient receptor potential (TRP) channels,[51] and these cells can couple with cardiomyocytes in the myocardium to regulate electrical properties and arrhythmogenesis.[51] Future studies are needed to investigate the potential alterations in fibroblast ion channels and their contributions to the reduced arrhythmogenesis in β-catenin KO hearts after MI.

In summary, this study demonstrated that deletion of β-catenin reduces ventricular tachyarrhythmias in post-MI hearts primarily through attenuated structural remodeling. However, this study only examined the ischemic heart failure mouse model, and future studies

are warranted to investigate the Wnt/β-catenin pathway activation in cardiomyocytes and its role in arrhythmogenesis in other types of heart failure, such as those induced by pressure overload or angiotensin II.[17-19]

References

1 Benjamin, E. J. et al. Heart Disease and Stroke Statistics-2018 Update: A Report From the American Heart Association. Circulation 137, e67-e492, doi:10.1161/cir.0000000000000558 (2018).

2 Chugh, S. S. Sudden cardiac death in 2017: Spotlight on prediction and prevention. Int J Cardiol 237, 2-5, doi:10.1016/j.ijcard.2017.03.086 (2017).

3 Zheng, Z. J., Croft, J. B., Giles, W. H. & Mensah, G. A. Sudden cardiac death in the United States, 1989 to 1998. Circulation 104, 2158-2163 (2001).

4 Roy, D. et al. Long-term reproducibility and significance of provokable ventricular arrhythmias after myocardial infarction. J Am Coll Cardiol 8, 32-39 (1986).

5 Marchlinski, F. E., Waxman, H. L., Buxton, A. E. & Josephson, M. E. Sustained ventricular tachyarrhythmias during the early postinfarction period: electrophysiologic findings and prognosis for survival. J Am Coll Cardiol 2, 240-250 (1983).

6 Jackson, N., Gizurarson, S., Massé, S. & Nanthakumar, K. in Cardiac Electrophysiology: From Cell to Bedside, 2018 (eds D. P. Zipes, J. Jalife, & W. G. Stevenson) Ch. 48.

7 Tomaselli, G. F. & Zipes, D. P. What causes sudden death in heart failure? Circ Res 95, 754-763, doi:10.1161/01.RES.0000145047.14691.db (2004).

8 Tomaselli, G. F. & Marbán, E. Electrophysiological remodeling in hypertrophy and heart failure. Cardiovasc Res 42, 270-283, doi:10.1016/s0008-6363(99)00017-6 (1999).

9 Pu, J. & Boyden, P. A. Alterations of Na+ currents in myocytes from epicardial border zone of the infarcted heart. A possible ionic mechanism for reduced excitability and postrepolarization refractoriness. Circ Res 81, 110-119 (1997).

10 Wit, A. L. & Peters, N. S. The role of gap junctions in the arrhythmias of ischemia and infarction. Heart Rhythm 9, 308-311, doi:10.1016/j.hrthm.2011.09.056 (2012).

11 Gilmour, R. F., Jr., Heger, J. J., Prystowsky, E. N. & Zipes, D. P. Cellular electrophysiologic abnormalities of diseased human ventricular myocardium. The American journal of cardiology 51, 137-144, doi:10.1016/s0002-9149(83)80024-1 (1983).

12 Gessert, S. & Kühl, M. The multiple phases and faces of wnt signaling during cardiac differentiation and development. Circ Res 107, 186-199, doi:10.1161/circresaha.110.221531 (2010).

13 Liang, W. et al. Canonical Wnt signaling promotes pacemaker cell specification of cardiac mesodermal cells derived from mouse and human embryonic stem cells. Stem Cells 38, 352-368, doi:10.1002/stem.3106 (2020).

14 Hou, N. et al. Transcription Factor 7-like 2 Mediates Canonical Wnt/beta-Catenin Signaling and c-Myc Upregulation in Heart Failure. Circ Heart Fail 9:e003010, doi:10.1161/CIRCHEARTFAILURE.116.003010 e003010 10.1161/circheartfailure.116.003010 (2016).

15 Duan, J. et al. Wnt1/betacatenin injury response activates the epicardium and cardiac fibroblasts to promote cardiac repair. Embo J 31, 429-442, doi:10.1038/emboj.2011.418 (2012).

16 Dawson, K., Aflaki, M. & Nattel, S. Role of the Wnt-Frizzled system in cardiac pathophysiology: a rapidly developing, poorly understood area with enormous potential. J Physiol 591, 1409-1432, doi:10.1113/jphysiol.2012.235382 (2013).

17 Iyer, L. M. et al. A context-specific cardiac β-catenin and GATA4 interaction influences TCF7L2 occupancy and remodels chromatin driving disease progression in the adult heart. Nucleic Acids Res 46, 2850-2867, doi:10.1093/nar/gky049 (2018).
18 Malekar, P. et al. Wnt signaling is critical for maladaptive cardiac hypertrophy and accelerates myocardial remodeling. Hypertension 55, 939-945, doi:10.1161/HYPERTENSIONAHA.109.141127 (2010).
19 Zhao, Y. et al. An essential role for Wnt/β-catenin signaling in mediating hypertensive heart disease. Sci Rep 8, 8996, doi:10.1038/s41598-018-27064-2 (2018).
20 Bergmann, M. W. WNT signaling in adult cardiac hypertrophy and remodeling: lessons learned from cardiac development. Circ Res 107, 1198-1208, doi:10.1161/circresaha.110.223768 (2010).
21 Borrell-Pages, M. et al. LRP5/canonical Wnt signaling and healing of ischemic myocardium. Basic Res Cardiol 111, 67, doi:10.1007/s00395-016-0585-y (2016).
22 Liang, W., Cho, H. C. & Marban, E. Wnt signaling suppresses voltage-dependent Na(+) channel expression in postnatal rat cardiomyocytes. J Physiol 593, 1147-1157 (2015).
23 Lu, A. et al. Direct and indirect suppression of Scn5a gene expression mediates cardiac Na+ channel inhibition by Wnt signaling. Can J Cardiol 36, 564-576, doi:https://doi.org/10.1016/j.cjca.2019.09.019 (2020).
24 Lu, A. et al. Inhibition of β-catenin Increases Voltage-gated Na + Current in Brugada Syndrome Cardiomyocytes (March 30, 2021). Available at SSRN: https://ssrn.com/abstract=3815857 or http://dx.doi.org/10.2139/ssrn.3815857 (2021).
25 Wang, N. et al. Activation of Wnt/beta-catenin signaling by hydrogen peroxide transcriptionally inhibits NaV1.5 expression. Free Radic Biol Med 96, 34-44, doi:10.1016/j.freeradbiomed.2016.04.003 (2016).
26 Zhao, L., Sun, L., Lu, Y., Li, F. & Xu, H. A small-molecule LF3 abrogates beta-catenin/TCF4-mediated suppression of NaV1.5 expression in HL-1 cardiomyocytes. J Mol Cell Cardiol 135, 90-96, doi:10.1016/j.yjmcc.2019.08.007 (2019).
27 Gillers, B. S. et al. Canonical wnt signaling regulates atrioventricular junction programming and electrophysiological properties. Circ Res 116, 398-406, doi:10.1161/CIRCRESAHA.116.304731 (2015).
28 Li, G. et al. Differential Wnt-mediated programming and arrhythmogenesis in right versus left ventricles. J Mol Cell Cardiol 123, 92-107, doi:10.1016/j.yjmcc.2018.09.002 (2018).
29 Hahn, J. Y. et al. Beta-catenin overexpression reduces myocardial infarct size through differential effects on cardiomyocytes and cardiac fibroblasts. J Biol Chem 281, 30979-30989, doi:10.1074/jbc.M603916200 (2006).
30 Oikonomopoulos, A. et al. Wnt signaling exerts an antiproliferative effect on adult cardiac progenitor cells through IGFBP3. Circ Res 109, 1363-1374, doi:10.1161/circresaha.111.250282 (2011).
31 Barandon, L. et al. Reduction of infarct size and prevention of cardiac rupture in transgenic mice overexpressing FrzA. Circulation 108, 2282-2289, doi:10.1161/01.cir.0000093186.22847.4c (2003).
32 Zelarayán, L. C. et al. Beta-Catenin downregulation attenuates ischemic cardiac remodeling through enhanced resident precursor cell differentiation. Proc Natl Acad Sci U S A 105, 19762-19767, doi:10.1073/pnas.0808393105 (2008).
33 Gharibeh, L. et al. GATA6 is a regulator of sinus node development and heart rhythm. Proc Natl Acad Sci U S A 118, doi:10.1073/pnas.2007322118 (2021).

34 Cruciat, C. M. & Niehrs, C. Secreted and transmembrane wnt inhibitors and activators. Cold Spring Harbor perspectives in biology 5, a015081, doi:10.1101/cshperspect.a015081 (2013).
35 Bao, J., Zheng, J. J. & Wu, D. The structural basis of DKK-mediated inhibition of Wnt/LRP signaling. Science signaling 5, pe22, doi:10.1126/scisignal.2003028 (2012). Valenta, T., Hausmann, G. & Basler, K. The many faces and functions of beta-catenin. *Embo J* **31**, 2714-2736, doi:10.1038/emboj.2012.150 (2012).
37 Wang, Z. *et al.* Wnt signaling activates MFSD2A to suppress vascular endothelial transcytosis and maintain blood-retinal barrier. *Sci Adv* **6**, eaba7457, doi:10.1126/sciadv.aba7457 (2020).
38 Yang, S. & Huang, X. Y. Ca2+ influx through L-type Ca2+ channels controls the trailing tail contraction in growth factor-induced fibroblast cell migration. *J Biol Chem* **280**, 27130-27137, doi:10.1074/jbc.M501625200 (2005).
39 Pride, Y. B. *et al.* Relation between myocardial infarct size and ventricular tachyarrhythmia among patients with preserved left ventricular ejection fraction following fibrinolytic therapy for ST-segment elevation myocardial infarction. *The American journal of cardiology* **104**, 475-479, doi:10.1016/j.amjcard.2009.04.005 (2009).
40 Alexandre, J. *et al.* Scar extent as a predictive factor of ventricular tachycardia cycle length after myocardial infarction: implications for implantable cardioverter-defibrillator programming optimization. *Europace* **16**, 220-226, doi:10.1093/europace/eut289 (2014).
41 Josephson, M. E., Horowitz, L. N. & Farshidi, A. Continuous local electrical activity. A mechanism of recurrent ventricular tachycardia. *Circulation* **57**, 659-665, doi:10.1161/01.cir.57.4.659 (1978).
42 Wang, N. C. *et al.* Clinical implications of QRS duration in patients hospitalized with worsening heart failure and reduced left ventricular ejection fraction. *Jama* **299**, 2656-2666, doi:10.1001/jama.299.22.2656 (2008).
43 Dhingra, R. *et al.* Electrocardiographic QRS duration and the risk of congestive heart failure: the Framingham Heart Study. *Hypertension* **47**, 861-867, doi:10.1161/01.hyp.0000217141.20163.23 (2006).
44 He, B. J., Boyden, P. & Scheinman, M. Ventricular arrhythmias involving the His-Purkinje system in the structurally abnormal heart. *Pacing and clinical electrophysiology : PACE* **41**, 1051-1059, doi:10.1111/pace.13465 (2018).
45 Puljevic, D., Smalcelj, A., Durakovic, Z. & Goldner, V. Effects of postmyocardial infarction scar size, cardiac function, and severity of coronary artery disease on QT interval dispersion as a risk factor for complex ventricular arrhythmia. *Pacing and clinical electrophysiology : PACE* **21**, 1508-1516, doi:10.1111/j.1540-8159.1998.tb00237.x (1998).
46 Deb, A. Cell-cell interaction in the heart via Wnt/β-catenin pathway after cardiac injury. *Cardiovasc Res* **102**, 214-223, doi:10.1093/cvr/cvu054 (2014).
47 Valenta, T., Hausmann, G. & Basler, K. The many faces and functions of β-catenin. *Embo J* **31**, 2714-2736, doi:10.1038/emboj.2012.150 (2012).
48 Zuppinger, C., Eppenberger-Eberhardt, M. & Eppenberger, H. M. N-Cadherin: structure, function and importance in the formation of new intercalated disc-like cell contacts in cardiomyocytes. *Heart failure reviews* **5**, 251-257, doi:10.1023/a:1009809520194 (2000).
49 Kuwabara, Y. *et al.* Increased expression of HCN channels in the ventricular myocardium contributes to enhanced arrhythmicity in mouse failing hearts. *J Am Heart Assoc* **2**, e000150, doi:10.1161/jaha.113.000150 (2013).

50 Hofmann, F. *et al.* Ventricular HCN channels decrease the repolarization reserve in the hypertrophic heart. *Cardiovasc Res* **95**, 317-326, doi:10.1093/cvr/cvs184 (2012).
51 Yue, L., Xie, J. & Nattel, S. Molecular determinants of cardiac fibroblast electrical function and therapeutic implications for atrial fibrillation. *Cardiovasc Res* **89**, 744-753, doi:10.1093/cvr/cvq329 (2011).
52 Percie du Sert, N. *et al.* The ARRIVE guidelines 2.0: Updated guidelines for reporting animal research. *Br J Pharmacol* **177**, 3617-3624, doi:10.1111/bph.15193 (2020).
53 Molgat, A. S. *et al.* Hyperglycemia inhibits cardiac stem cell-mediated cardiac repair and angiogenic capacity. *Circulation* **130**, S70-76, doi:10.1161/circulationaha.113.007908 (2014).
54 Kapoor, N., Liang, W., Marban, E. & Cho, H. C. Direct conversion of quiescent cardiomyocytes to pacemaker cells by expression of Tbx18. *Nat Biotechnol* **31**, 54-62, doi:10.1038/nbt.2465 (2013).
55 Liang, W. *et al.* Role of phosphoinositide 3-kinase {alpha}, protein kinase C, and L-type Ca2+ channels in mediating the complex actions of angiotensin II on mouse cardiac contractility. *Hypertension* **56**, 422-429 (2010).
56 Jadhav, A. *et al.* Catharanthine dilates small mesenteric arteries and decreases heart rate and cardiac contractility by inhibition of voltage-operated calcium channels on vascular smooth muscle cells and cardiomyocytes. *J Pharmacol Exp Ther* **345**, 383-392, doi:10.1124/jpet.112.199661 (2013).

Acknowledgements

This work was supported by the Canadian Institutes of Health Research (Grant number: PJT-148918, to W.L.), McDonald Scholarship and New Investigator Award from Heart and Stroke Foundation of Canada (Grant number: S-17-LI-0866, to W.L.), a Scholarship (to J.W.) and a Postdoctoral Fellowship (to A.L.) from the University of Ottawa Cardiac Endowment Funds at the Heart Institute. Figures 1A, 1B, 1E, 5A, 5B and part of Figure 7A were created with BioRender.com with approved publication licenses.

Author contributions

J.W. and W.L conceived the experiments. J.W., Y.X., A.L., and H.W. performed experiments. J.W., D.R.D., P.L., R.S.B. and W.L. analyzed and interpreted results and wrote the manuscript. All authors reviewed and approved the manuscript.

Additional information

The authors declare that there is no competing interest.

Figure Legends:

Figure 1. β-catenin knockout reduces the susceptibility to ventricular tachycardias after myocardial infarction.

A. To generate cardiomyocyte-specific β-catenin (*Ctnnb1*) knockout mice, *Ctnnb1*$^{flox/flox}$ mice (with exons 2 to 6 floxed) were crossbred with αMHC-MerCreMer mice to obtain *Ctnnb1*$^{flox/flox}$;αMHC-MerCreMer$^{+/-}$ mice, which were then treated with tamoxifen for deletion of exons 2-6 generating *Ctnnb1* null allele due to the loss of the translational start site. Littermate *Ctnnb1*$^{flox/flox}$;αMHC-MerCreMer$^{-/-}$ mice were used as control wild-type mice.

B. Experimental design.

C. Representative western blot for confirmation of reduced total β-catenin in both sham and LAD-ligated (MI) KO hearts. Protein samples were prepared from left ventricular free wall of sham mice and from the border zone in mice at 8-weeks post-MI (myocardial infarction). GAPDH was used as a loading control. The original uncropped gel images are included in Supplementary Figure 1.

D. Survival curve showing no difference in survival between WT and KO mice after LAD ligation (p=0.7473, analyzed by Log-rank (Mantel-Cox) test). Only the mice in the long-term (8-weeks after MI) study were included in this survival analysis. All mortality occurred within the first week.

E. Protocols for evaluation of the inducibility of ventricular tachyarrhythmias (VT).

Left Panel: Mouse hearts were isolated and Langendorff-perfused with Tyrode solution containing isoproterenol, *ex vivo* ECG were continuously measured by placing recording electrodes around the heart as we previously described.[20,46] Programmed electrical stimulation

(PES) was applied using a MyoPacer (IonOptix) via a pair of platinum electrodes placed on the left ventricular apex of the heart.

Right Panel: the standard stimulation protocol consisted of 10 stimuli at 100 ms intervals (S1, 5V) followed by one extra stimulus (S2) starting at an interval of 80 ms which was then reduced by 2 ms until the effective refractory period (ERP) was reached. If VT or VF was not induced, a second extra stimulus (S3) was added at 80 ms after S2. The S3 interval was then reduced by 2 ms until the ERP was reached. Finally, a third extra stimulus (S4) was added 80 ms after S3 and was then decreased by 2 ms until the ERP was reached. If a heart failed to develop a VT or VF with 3 extra stimuli, the heart was deemed non-inducible.

F. Representative *ex vivo* ECG (Lead II) showing PES-induced ventricular tachycardia (defined as 3 or more consecutive PVCs) in a WT heart (8-week after MI) when stimulated with one extra stimulus (S2), and only one single PVC in a KO heart (8-week after MI) when stimulated with three extra stimuluses (S4).

G. Summary of PES-induced PVCs and VTs in WT and KO hearts at 1 or 8 weeks after MI. An arrhythmia score was assigned to each heart according to the criteria shown in the left table.

At 8 weeks after MI, VT was successfully induced in 77% of WT hearts but only in 18% of KO hearts. Data were analyzed by two-way ANOVA and Bonferroni *post-hoc* comparison.

Figure 2. β-catenin knockout reduces the prolongation of QRS duration and QT interval after myocardial infarction.

A. Representative *in vivo* surface ECG traces (Lead II) in sham mice (left) and in mice at 8 weeks after MI (right).

B. Summary of *in vivo* ECG parameters, including QT Interval (top left), QRS duration (top right), PR Interval (bottom left), and RR Interval (bottom right). n=10-13 per group. *p<0.05, **p<0.01, vs. corresponding sham groups; $^{\#}$p<0.05, $^{\#\#}$p<0.01, vs. WT MI group at the indicated timepoints. Data were analyzed by two-way ANOVA and Bonferroni *post-hoc* comparison.

Figure 3. β-catenin knockout attenuates pump dysfunction and chamber dilation after myocardial infarction.

A. Representative short axis, M-mode echocardiographic recordings at the left ventricular mid-papillary level showing attenuation of cardiac function and dilation in β-catenin KO mice post-MI. Echocardiogram was recorded when heart rates were in the 400-500 bpm range.

B to D. Summary of echocardiographic parameters of mice up to 8 weeks after MI showing reduced left ventricular dilation in KO mice as measured by end diastolic volume (EDV, panel B, left) and end systolic volume (ESV, panel B, right), attenuation of cardiac systolic dysfunction in KO mice as measured by ejection fraction (panel C, left) and fractional shortening (panel C, right), and unchanged left ventricular posterior wall thickness at diastole (LVPWd, panel D, left) and at systole (LVPDs, panel D, right). n=10-13 per group. *p<0.05, **p<0.01, vs. corresponding sham groups; $^{\#}$p<0.05, $^{\#\#}$p<0.01, vs. WT MI group at the indicated timepoints. Data were analyzed by two-way ANOVA and Bonferroni *post-hoc* comparison.

Figure 4. β-catenin knockout reduces scar sizes after myocardial infarction.

A. Representative images of Masson's trichrome staining of mouse heart tissue sections at 5 different levels from LAD ligation site (top) to the apex (bottom) at 8 weeks after MI (right), as well as in sham-operated hearts (left). The scar size for each the 5 different levels was calculated

as the percentage of fibrotic area (as indicated by the arrows) to the total area of the left ventricle section. The heart's total scar size was then calculated as the mean of the scar sizes at the 5 levels and reported in panel B.

B. Summary of scar size showing reduced scar size in KO hearts (n=5) compared to WT hearts (n=6). Statistical analysis was performed with a two-tailed unpaired t-test.

Figure 5. Upregulation of Wnt agonists and antagonists in myocardial tissues after myocardial infarction.

A. Diagram of the canonical Wnt/β-catenin signaling pathway, which is fine-tuned by the soluble Wnt ligands (green color) and Wnt inhibitors (red color) on the extracellular side of the plasma membrane. When a Wnt ligand binds to its plasma membrane receptor (purple color) and co-receptor (blue color), it leads to the inhibition of GSK-3β which is the key component of the β-catenin degradation complex; β-catenin will accumulate in the cytoplasm and then translocate into the nucleus where it, together with TCF/LEF, activate or inhibit the transcription of target genes. *Abbreviations*: GSK-3β, glycogen synthase kinase 3β; TCF/LEF, T-cell factor/lymphoid enhancer factor.

B. Detection of gene transcript levels from RNA samples extracted from heart tissues, which contained different cell types, such as cardiomyocytes (pink color), fibroblasts (brown color) and inflammatory cells (blue color). C and D. qRT-PCR analyses of transcript levels of Wnt ligands (C) and Wnt inhibitors (D) in sham, 1-week post MI, and 8-week post MI infarct and border zone myocardium. n=4-10 per group. *$p<0.05$ vs. corresponding sham groups. "ns" means no significant difference between WT and KO groups. Data were analyzed by two-way ANOVA and Bonferroni *post-hoc* comparison.

Figure 6. Upregulation of Wnt receptors and co-receptors in myocardial tissues after myocardial infarction.

A and B. qRT-PCR analyses of transcript levels of Wnt receptors (A) and Wnt co-receptors (B) in sham, 1-week post MI, and 8-week post MI infarct and border zone myocardium. n=4-10 per group.

C. Western blot of border zone tissue (MI, n=5-6) or left ventricular anterior free wall (sham, n=5-6) with anti-non-phospho (active) β-catenin (Ser33/Ser37/Thr41) antibody and anti-total β-catenin antibody. GAPDH was used as a loading control. The original uncropped gel images are included in Supplementary Figure 1.

*$p<0.05$ vs. corresponding sham groups. "ns" means no significant difference between WT and KO groups. Data were analyzed by two-way ANOVA and Bonferroni *post-hoc* comparison.

Figure 7. Upregulation of Wnt pathway genes in purified cardiomyocytes after myocardial infarction.

A. Isolation of pure cardiomyocytes from mouse hearts. Mouse hearts were digested with collagenase on a Langendorff perfusion system. The infarct and border region (or the left ventricular free wall in sham groups) were dissected, cut into small pieces, and gently pipetted to release single cells. The cell suspension contained both cardiomyocytes (rod-like cells) and other cell types (the Hoechst-positive small round cells), which can be separated by their different settlement speed: after a 10-min settlement, the cardiomyocytes were enriched in the pellet while the other cell types (non-cardiomyocytes) remained in the supernatant. The pellet containing pure cardiomyocytes was used for RNA extraction and qPCR analysis. The Hoechst-negative small particles are likely cell debris.

B to D. qRT-PCR analyses of transcript levels of Wnt ligands (B), Wnt inhibitors (C) and Wnt receptors and coreceptors genes (D) in pure cardiomyocytes isolated from sham, 1-week post MI, and 6-week post MI infarct and border zone. n=3-6 per group. *p<0.05 vs. corresponding sham groups. "ns" means no significant difference between WT and KO groups. Data were analyzed by two-way ANOVA and Bonferroni *post-hoc* comparison.

Figure 8. Ion channel gene expressions after myocardial infarction.

A and B. qRT-PCR analyses of transcript levels of ion channels involved in ventricular action potentials (A), and gap junctions and HCN channels (B) in sham, 1-week post MI, and 8-week post MI infarct and border zone myocardium. n=4-10 per group. *p<0.05 vs. corresponding sham groups. "ns" means no significant difference between WT and KO groups. Data were analyzed by two-way ANOVA and Bonferroni post-hoc comparison. Abbreviations in panel A: I_{Na}, cardiac sodium current; Ito, transient outward potassium current; $I_{Ca,L}$, L-type calcium current, I_{Kr}, rapidly activating delayed rectifier potassium current; IKs, slowly activating delayed rectifier potassium current; IK1, inwardly rectifying potassium current.

C. Representative confocal images showing similar distribution patterns of Connexin 43 (Cx43, green) in WT and KO myocardium. In sham hearts (top panels) of both WT and KO groups, Cx43 is restricted to the cell-cell junctions. In the border zone of hearts at 8-week after MI (bottom panels), both WT and KO groups showed a more diffusive pattern for Cx43. Cells were co-stained with α-sarcomeric actinin (α-SA, red color, a marker of cardiomyocytes) and DAPI (blue).

Figure 1. β-catenin knockout reduces the susceptibility to ventricular tachycardias after myocardial infarction

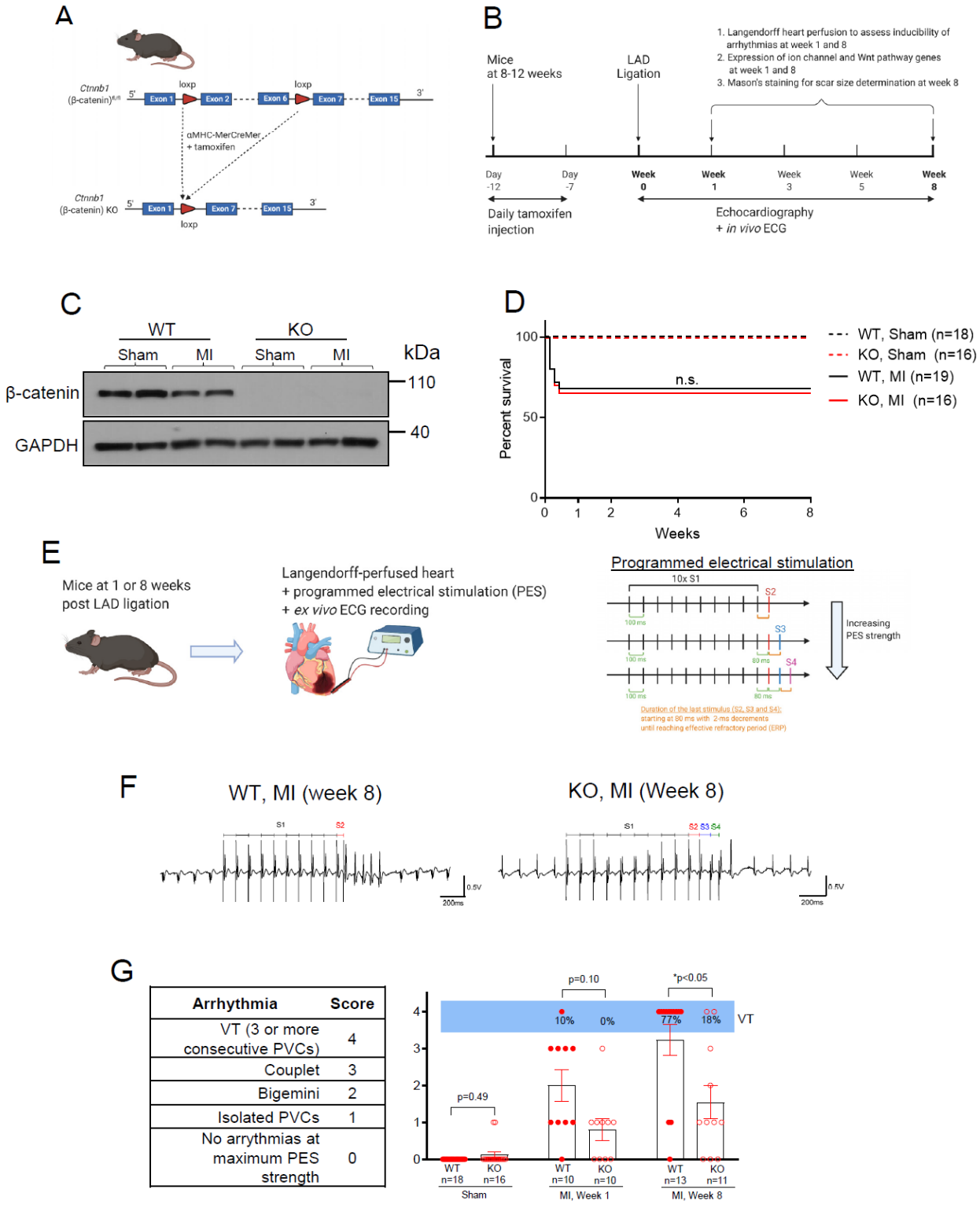

Arrhythmia	Score
VT (3 or more consecutive PVCs)	4
Couplet	3
Bigemini	2
Isolated PVCs	1
No arrythmias at maximum PES strength	0

Figure 2. β-catenin knockout prevents the prolongation of QRS duration and QT interval after myocardial infarction

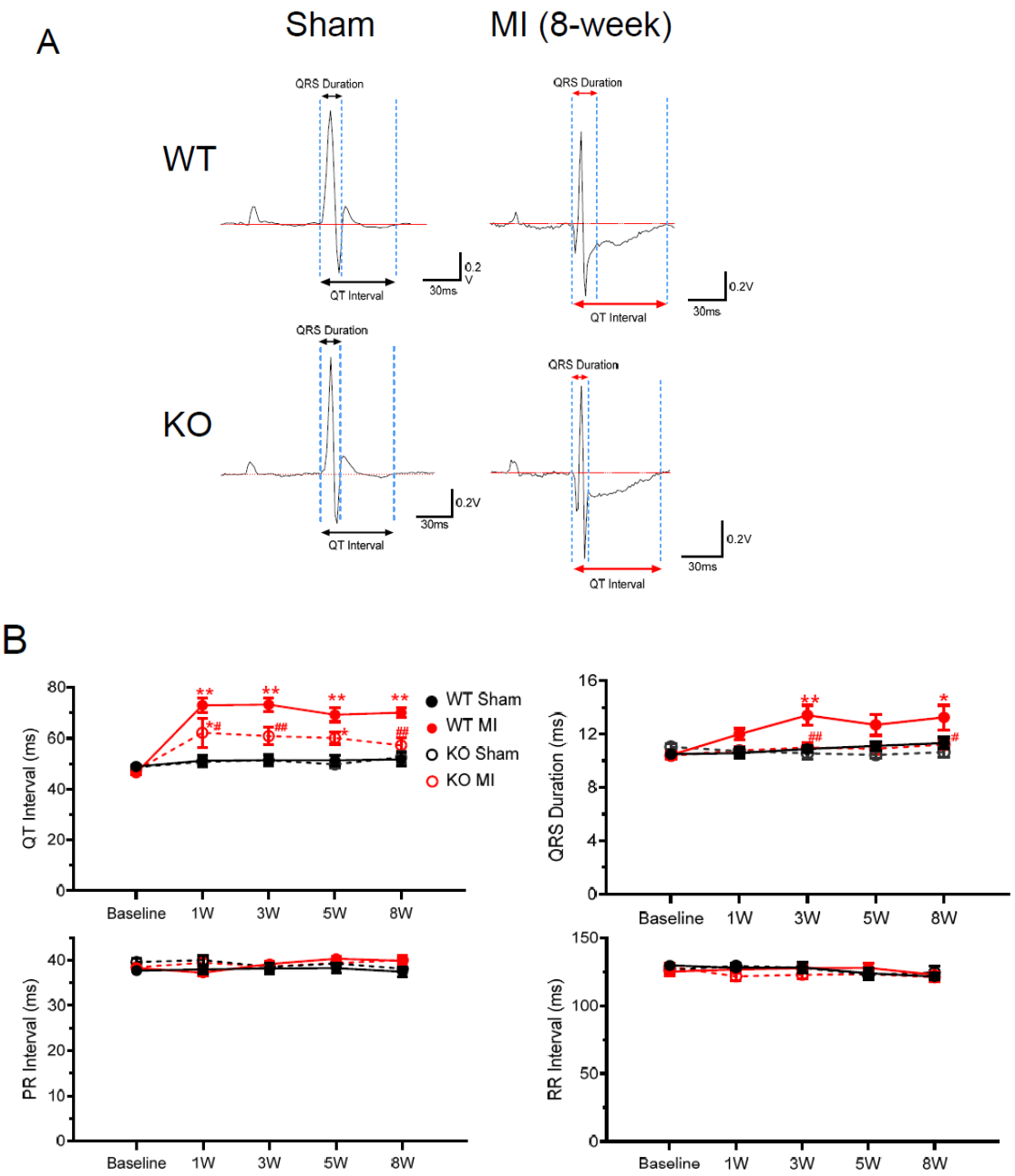

Figure 3. β-catenin knockout attenuates pump dysfunction and chamber dilation after myocardial infarction

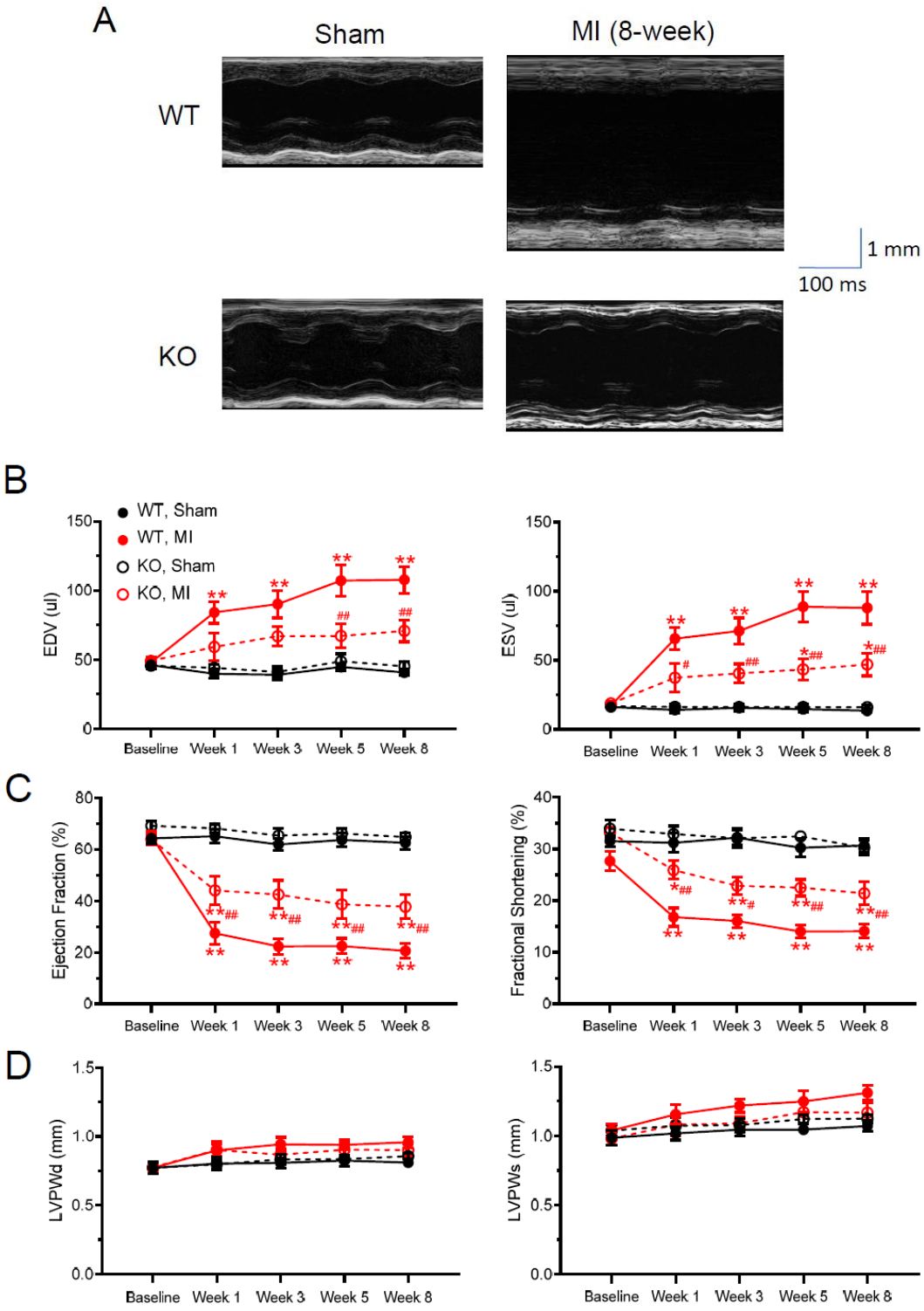

Figure 4. β-catenin knockout reduces scar sizes after myocardial infarction

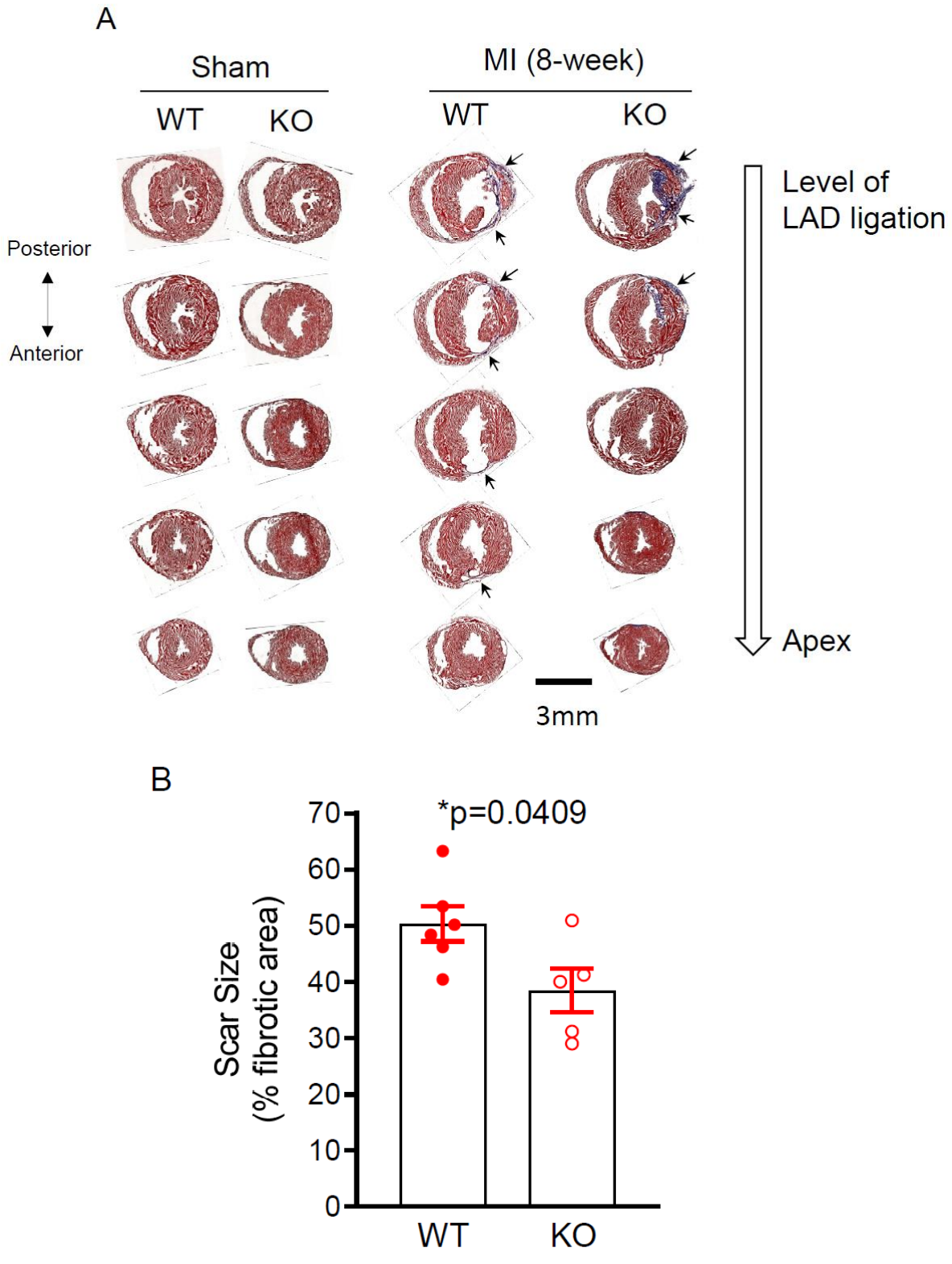

Figure 5. Both Wnt agonists and antagonists are upregulated after myocardial infarction

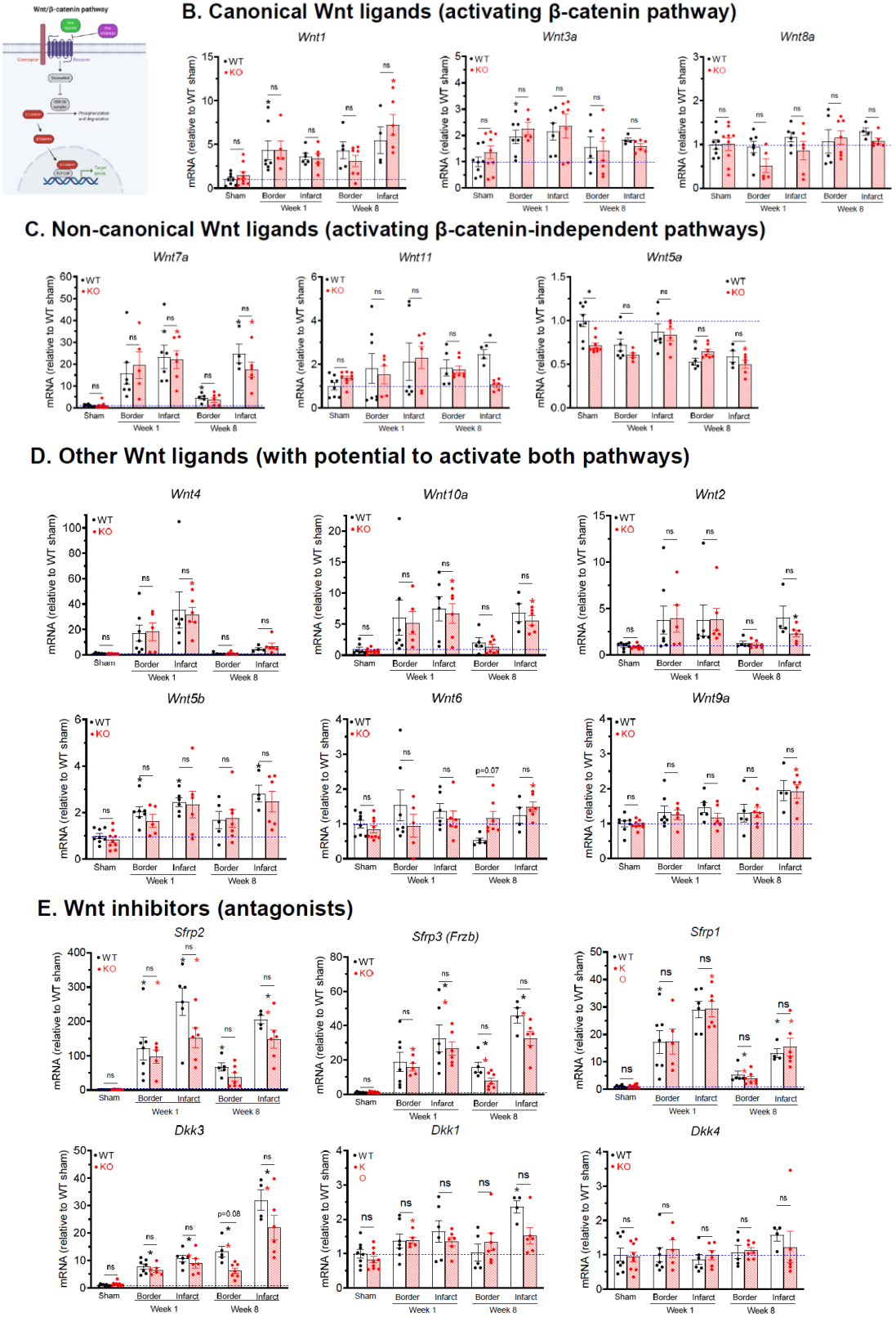

Figure 6. Wnt receptors and co-receptors are upregulated after myocardial infarction

A. Wnt receptors (Frizzled, Fzd)

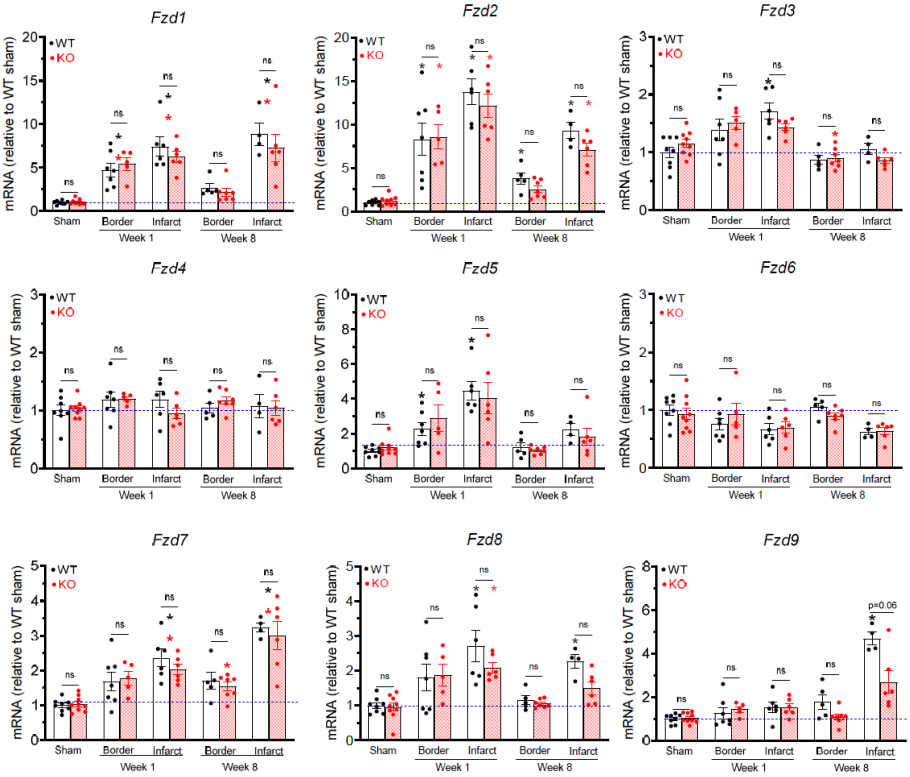

B. Wnt co-receptors

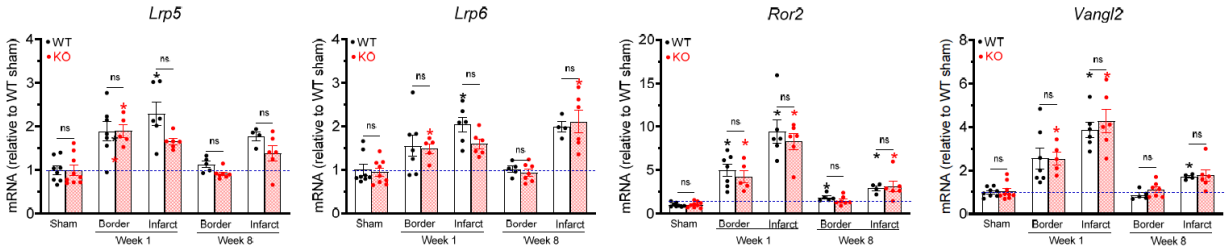

C. β-catenin protein

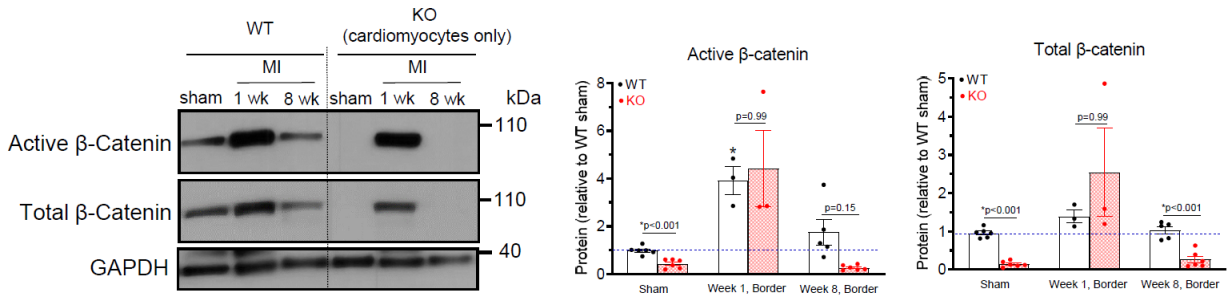

Figure 7

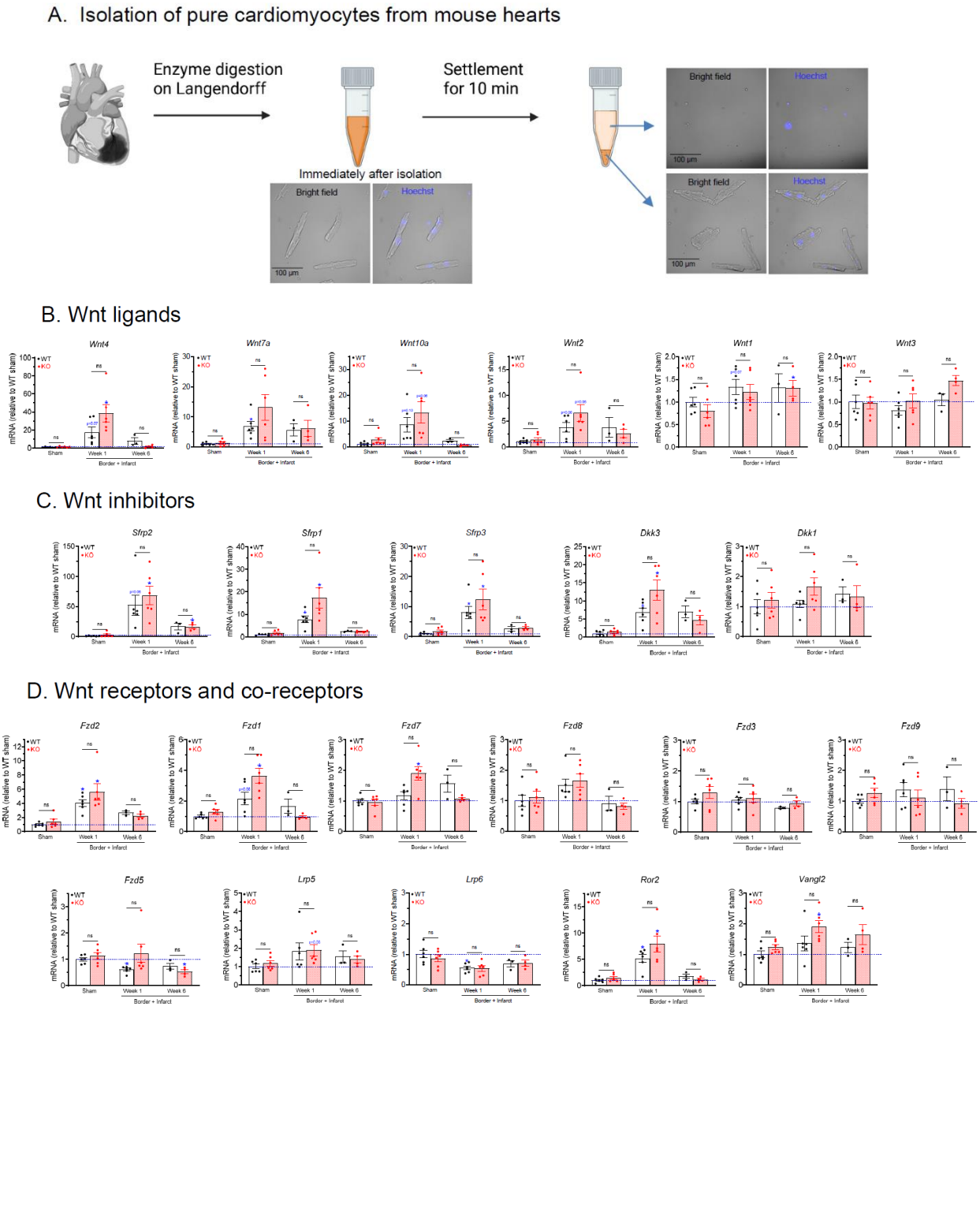
A. Isolation of pure cardiomyocytes from mouse hearts
Enzyme digestion on Langendorff
Settlement for 10 min
Immediately after isolation
Bright field
Hoechst
100 µm
B. Wnt ligands
Wnt4
Wnt7a
Wnt10a
Wnt2
Wnt1
Wnt3
C. Wnt inhibitors
Sfrp2
Sfrp1
Sfrp3
Dkk3
Dkk1
D. Wnt receptors and co-receptors
Fzd2
Fzd1
Fzd7
Fzd8
Fzd3
Fzd9
Fzd5
Lrp5
Lrp6
Ror2
Vangl2
mRNA (relative to WT sham)
WT
KO
Sham
Week 1
Week 6
Border + Infarct

Figure 8

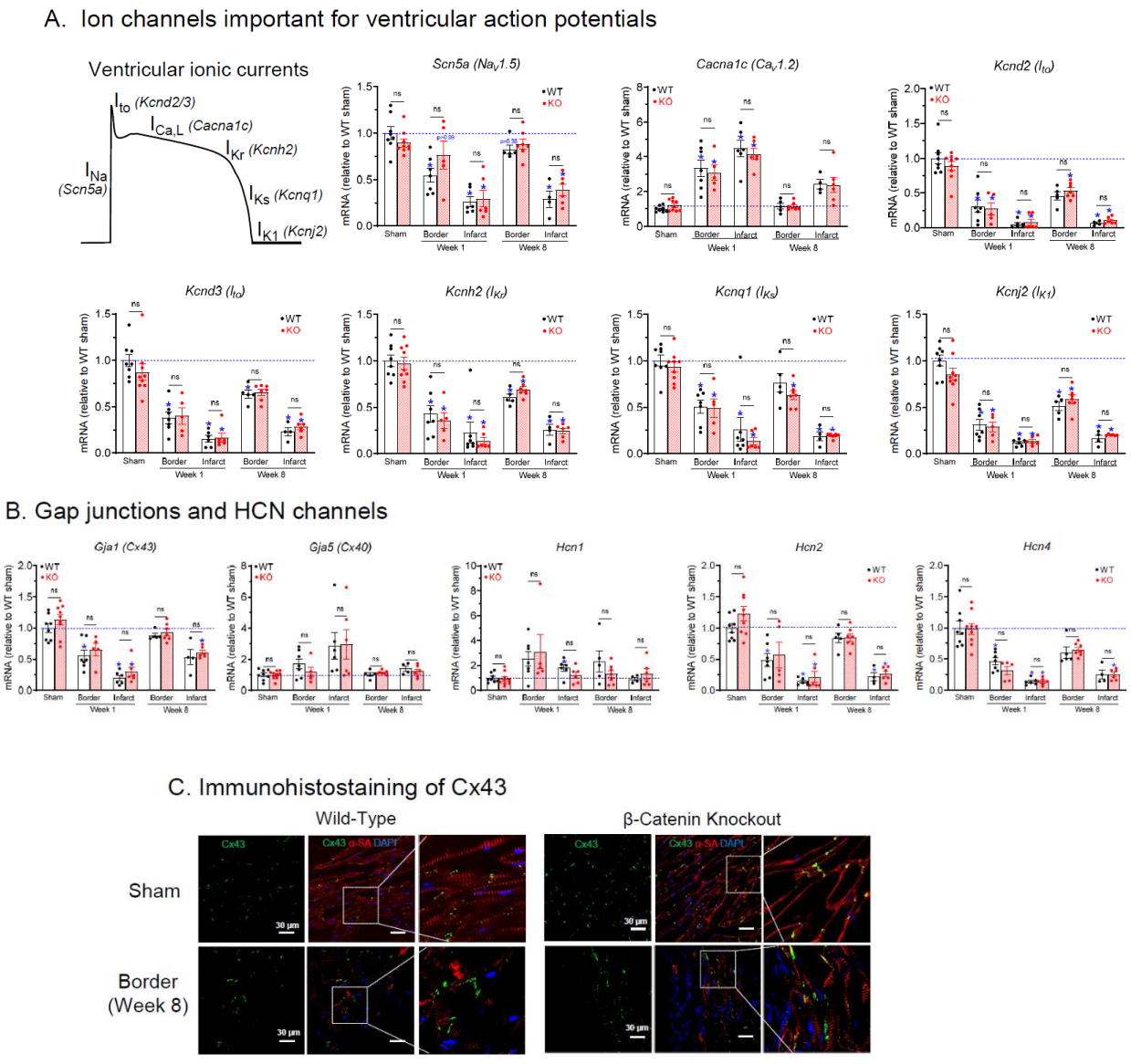
A. Ion channels important for ventricular action potentials
Ventricular ionic currents
Ito (Kcnd2/3)
ICa,L (Cacna1c)
IKr (Kcnh2)
INa (Scn5a)
IKs (Kcnq1)
IK1 (Kcnj2)
Scn5a (Nav1.5)
Cacna1c (Cav1.2)
Kcnd2 (Ito)
Kcnd3 (Ito)
Kcnh2 (IKr)
Kcnq1 (IKs)
Kcnj2 (IK1)
mRNA (relative to WT sham)
WT
KO
Sham
Border
Infarct
Week 1
Week 8
B. Gap junctions and HCN channels
Gja1 (Cx43)
Gja5 (Cx40)
Hcn1
Hcn2
Hcn4
C. Immunohistostaining of Cx43
Wild-Type
β-Catenin Knockout
Sham
Border (Week 8)
Cx43
Cx43 α-SA DAPI
30 μm

Supplementary Figure 1. Original uncropped gel images for Figure 1C and 6C.

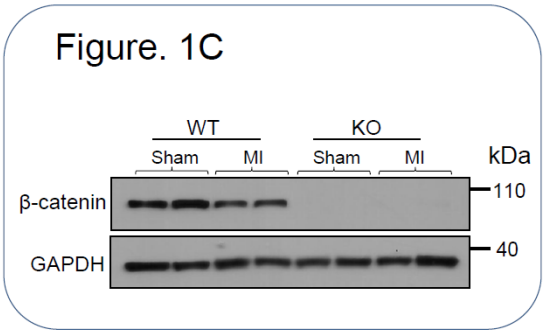

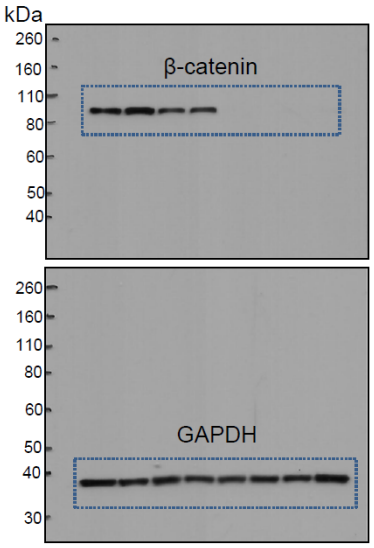

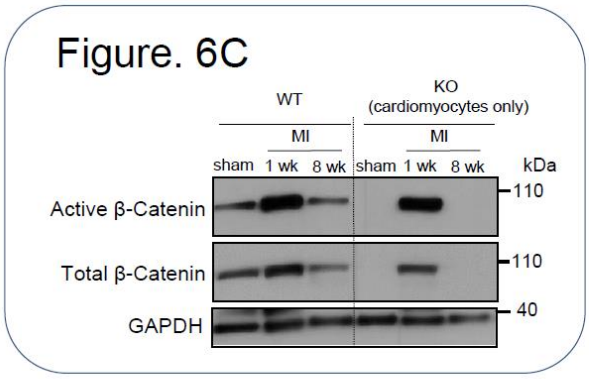

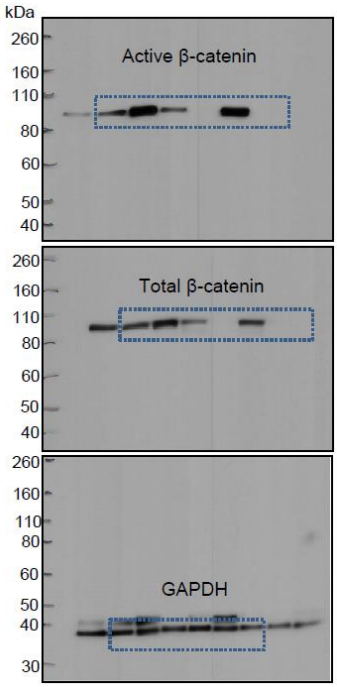

Table 1. Primers for SYBR green qPCR analysis of mouse heart tissues.

Gene	Forward sequence (5' - 3')	Reverse Sequence (5' - 3')	Amplicon Size (bp)	Target exon(s)
Wnt1	AGGGCGAACGACCGTGT	TCGGTTGCCGTAAAGGACG	169	3-4
Wnt2	GACCTGATGTAGACGCAAGGG	TGTAGCTCTCATGTACCACCAT	127	1-2
Wnt2b	ACACGTCCTGGTGGTACATAG	ATGTCTGGGTAGCGTTGACA	107	1-2
Wnt3	TGTTCCAACTATTGGGGGCG	GGCCAGGGACCACCAAAT	163	1-2
Wnt3a	CTACCCGATCTGGTGGTCCT	ACAGAGAATGGGCTGAGTGC	70	1-2
Wnt4	CGAGCAATTGGCTGTACCTGG	GTTTCTCGCACGTCTCCTCT	72	1-2
Wnt5a	GCTTTGGATTGTCCCCCAAG	ATTCCAATGGGCTTCTTCATGG	123	1-2
Wnt5b	GTTCCCTGAATGGCGGCTA	AGAGCTAGTGACCACCAGGA	179	1-2
Wnt6	TTCCAGTTCCGTTTCCGACG	CTGTCTCTCGGATGTCCTGC	85	2-3
Wnt7a	GAGATCAAGCAGAATGCCCG	TTCTCCTCCAGGATCTTCCGA	74	3-4
Wnt7b	CCTAGGAAGGCCAGTGACCA	CACGGATGACAATGCTCTGTAAG	153	1-2
Wnt8a	GCCTATCTGACCTACACCGC	GATGTCTCTCTCGTGGCAGC	155	3-4
Wnt9a	CCTCGTGGGTGTGAAGGTGATA	CTTCATTGGTAGTGCTGCCC	179	3-4
Wnt10a	CATCTTCAGCCGAGGTTTTCG	AGCCTTCAGTTTACCCAGAGC	106	2-3
Wnt11	GCAACCTCGCAGGCGG	CAAGGCAAAGAGCAGAGCCT	157	2-3
Fzd1	ACGAGGCTTACCAACAGCAA	CAGGCGATGGCTAGGATCAG	93	1
Fzd2	CCTCAAGGTGCCGTCCTATC	CAACACCGACCATGTGAGGA	151	1
Fzd3	GCAGATAGGTGGGCACAGTT	ATAGGGTGGAAGGGCTCCAT	150	2-3
Fzd4	TTCGGGGACGAGGAGGAG	ACCGAACAAAGGAAGAACTGC	194	1-2
Fzd5	TGTCGTTAAACTTTCCCAGCTCT	CTCCAAGGACAGAACTCTCGGA	113	1-2
Fzd6	CGGAGCCGCAGCAGTT	GGGACCTTTCCATCTTGCCA	186	1-2
Fzd7	TACGTGGGCCTGTCTAGTGT	CTTCTCTGTCTTGGTGCCGT	156	1
Fzd8	CCGCCTAGAGAAGGAGGACT	GAGCGAGGTCACTTCCAACA	75	1
Fzd9	CGTCGAGGTGTTCTGGTCTC	GAAGAAACACAACGCGGACC	79	1
Lrp5	TGCTCCCACATCTGTATCGC	AGGTAGGAGGCTCACCACAA	106	17-18
Lrp6	CTGCTGAGAGCGGCCC	CCAAACACAAAGTCCACCGC	137	1-2
Vangl2	GGGAAACAGGCGAGTGGTCT	GCAGCTCCCCGCCACT	196	1-2
Ror2	CTTCCCACTCTGAAAGGCTACT	CTTCGTGGCTCTTGCACAAC	164	1-2
Dkk1	CTCTTGACAACTACCAGCCCT	AGCACATAGCGTGCCTCAT	162	1-2
Dkk3	CATAAGCGTGTCAAGTGGAGC	GGAGTCCAAGTGACCGTCG	145	1-2
Dkk4	ACAAAGCAGTAAGGGACAGGA	TCCCTCTCGTAGAACTGGCT	118	3-4
Sfrp1	GCAAGCGAGTTTGCACTGAG	CCGCTTCAGCTCCTTCTTCT	126	2-3
Sfrp2	GCCACAGAGGAAGCTCCCAAG	GACACGCCGTTCAGCTTGTAA	194	1-3
Frzb	GCCGTTGTGGAAGTGAAGGA	GCCTTCTACCAAGAGTAACCTGG	174	4-5
Axin2	GGCAACTCAGTAACAGCCCAA	GCTCATGTGAGCCTCCTCTCTTT	139	1-2
Tcf7l2	AATCCACCTCCGCACTTACC	GGCTGACCTTGCTGTGGT	158	5-7

4. Conclusions, Limitations, and Future Directions

Our results demonstrated that β-catenin knockout in cardiomyocytes is associated with reduced arrhythmia risk in mouse hearts after myocardial infarction. Although Wnt/β-catenin signaling is capable of regulating ion channel genes in cardiomyocytes, our results suggest that this signaling is not activated in cardiomyocytes at the subacute and chronic stages after myocardial infarction. This is consistent with the lack of differences in the cardiac ion channel genes between wild-type and cardiomyocyte-specific β-catenin knockout (KO) mice. Instead, the reduced susceptibility to arrhythmias in post-MI KO hearts is likely secondary to attenuated cardiac structural remodeling. These findings would also not support the use of Wnt inhibitors or other pharmacological blockers of the Wnt/β-catenin signaling cascade following an MI.

Further studies are warranted to investigate 1) whether the ion channel currents in the ventricular myocytes, to be recorded with whole-cell patch-clamp technique, of post-MI hearts are different between WT and KO mice. Although our qPCR suggested no difference in ion channel gene transcript, the potential effects of β-catenin inhibition on channel protein modification, function, and turnover should be investigated. 2) whether the mechanism of VTs, to be studied with optical mapping, is different in post-MI hearts between WT and KO mice. Using an optical mapping system, we would be able to measure any differences in ventricular conduction velocity and accurately determine the arrhythmia mechanism in our knockout mice. 3) If there is a sex-linked effect on death, arrhythmias, and electrophysiological properties. Although we have conducted an analysis of sex effects on the data in the current study and found no differences, the sample numbers were not large enough to confidently conclude that there is in fact no link to sex between any of the parameters above.

Another important unanswered question is what are the mechanisms underlying the attenuated structural remodeling (i.e. smaller scar size) in post-MI KO mice? Studies are needed to investigate 1) if myocyte apoptosis/survival, angiogenesis, and fibrosis are different in post-MI hearts between WT and KO mice. These studies will provide critical information for understanding the cardioprotective effects of β-catenin inhibition and guide the future development of therapeutic strategies for myocardial infarction. 2) Protein expression and modifications of various targets (Wnt signaling components, ion channel subunits, gap junction proteins), as assessed by western blotting in the whole tissue lysates and in isolated cell populations, would provide further insight into possible differences between the WT and KO groups that may explain the reduced susceptibility to arrhythmias. 3) When the difference between WT and KO mice first begins to develop (since we only tested the week 1 and 8 timepoints), and what critical stages in the remodeling process this may correspond with to guide future studies into possible interventional strategies.

Our present findings also did not investigate any factors that may have been related to the early deaths (1-3 days) following MI. Thus, our results may be subjected to a survivor selection bias, and there also may have been some molecular changes brought about by the β-catenin knockout that were not captured in these mice that died too soon following the surgery.

Additionally, future studies are needed to investigate the activation of Wnt/β-catenin signaling and ion channel remodeling in other forms of heart failure, such as those induced by pressure overload using a transverse aortic constriction (TAC) mouse model. In contrast to the conflicting results reported for Wnt activities in MI-induced heart failure, the TAC-induced cardiac hypertrophy and heart failure have been reported to have consistently increased Wnt/β-

catenin signaling (Malekar, 2010; Iyer, 2018), which would be a good disease model to test our hypothesis.

5. References

Adabag, A. S., Luepker, R. V., Roger, V. L., & Gersh, B. J. (2010). Sudden cardiac death: Epidemiology and risk factors. In *Nature Reviews Cardiology* (Vol. 7, Issue 4, pp. 216–225). NIH Public Access. https://doi.org/10.1038/nrcardio.2010.3

Ai, Z., Fischer, A., Spray, D. C., Brown, A. M. C., & Fishman, G. I. (2000). Wnt-1 regulation of connexin43 in cardiac myocytes. *Journal of Clinical Investigation*, *105*(2), 161–171. https://doi.org/10.1172/JCI7798

Alexandre, J., Saloux, E., Lebon, A., Dugué, A. E., Lemaitre, A., Roule, V., Labombarda, F., Champ-Rigot, L., Gomes, S., Pellissier, A., Scanu, P., & Milliez, P. (2014). Scar extent as a predictive factor of ventricular tachycardia cycle length after myocardial infarction: Implications for implantable cardioverter- defibrillator programming optimization. *Europace*, *16*(2), 220–226. https://doi.org/10.1093/europace/eut289

Arce, L., Pate, K. T., & Waterman, M. L. (2009). Groucho binds two conserved regions of LEF-1 for HDAC-dependent repression. *BMC Cancer*, *9*. https://doi.org/10.1186/1471-2407-9-159

Archbold, H. C., Yang, Y. X., Chen, L., & Cadigan, K. M. (2012). How do they do Wnt they do?: Regulation of transcription by the Wnt/β-catenin pathway. In *Acta Physiologica* (Vol. 204, Issue 1, pp. 74–109). Acta Physiol (Oxf). https://doi.org/10.1111/j.1748-1716.2011.02293.x

B, G., C, B. L., J, B. T., AJ, C., G, H., K, H., P, K., KH, K., G, K., T, L., A, R., M, S., RR, T., M, V., MA, V., C, V., U, Z., & SB, K. (2015). Cardiac arrhythmias in acute coronary syndromes: position paper from the joint EHRA, ACCA, and EAPCI task force. *EuroIntervention : Journal of EuroPCR in Collaboration with the Working Group on Interventional Cardiology of the European Society of Cardiology*, *10*(9), 1095–1108. https://doi.org/10.4244/EIJY14M08_19

B, R., I, A., E, P., C, F., S, M., & P, P. (1996). Binding of GSK3beta to the APC-beta-catenin complex and regulation of complex assembly. *Science (New York, N.Y.)*, *272*(5264), 1023–1026. https://doi.org/10.1126/SCIENCE.272.5264.1023

Barandon, L., Couffinhal, T., Ezan, J., Dufourcq, P., Costet, P., Alzieu, P., Leroux, L., Moreau, C., Dare, D., & Duplàa, C. (2003). Reduction of Infarct Size and Prevention of Cardiac Rupture in Transgenic Mice Overexpressing FrzA. *Circulation*, *108*(18), 2282–2289. https://doi.org/10.1161/01.CIR.0000093186.22847.4C

Barandon, L., Couffinhal, T., Ezan, J., Dufourcq, P., Costet, P., Alzieu, P., Leroux, L., Moreau, C., Dare, D., & Duplàa, C. (2003). Reduction of Infarct Size and Prevention of Cardiac

Rupture in Transgenic Mice Overexpressing FrzA. *Circulation*, *108*(18), 2282–2289. https://doi.org/10.1161/01.CIR.0000093186.22847.4C

Barker, N., Huch, M., Kujala, P., Wetering, M. van de, Snippert, H. J., Es, J. H. van, Sato, T., Stange, D. E., Begthel, H., Born, M. van den, Danenberg, E., Brink, S. van den, Korving, J., Abo, A., Peters, P. J., Wright, N., Poulsom, R., & Clevers, H. (2010). Lgr5+ve Stem Cells Drive Self-Renewal in the Stomach and Build Long-Lived Gastric Units In Vitro. *Cell Stem Cell*, *6*(1), 25–36. https://doi.org/10.1016/J.STEM.2009.11.013

Barker, N., van Es, J. H., Kuipers, J., Kujala, P., van den Born, M., Cozijnsen, M., Haegebarth, A., Korving, J., Begthel, H., Peters, P. J., & Clevers, H. (2007). Identification of stem cells in small intestine and colon by marker gene Lgr5. *Nature 2007 449:7165*, *449*(7165), 1003–1007. https://doi.org/10.1038/nature06196

Bhar-Amato, J., Davies, W., & Agarwal, S. (2017). Ventricular arrhythmia after acute myocardial infarction: "The perfect storm." *Arrhythmia and Electrophysiology Review*, *6*(3), 134–139. https://doi.org/10.15420/aer.2017.24.1

Borrell-Pages, M., Vilahur, G., Romero, J. C., Casaní, L., Bejar, M. T., & Badimon, L. (2016). LRP5/canonical Wnt signaling and healing of ischemic myocardium. *Basic Research in Cardiology*, *111*(6), 1–15. https://doi.org/10.1007/s00395-016-0585-y

Borrell-Pages, M., Vilahur, G., Romero, J. C., Casaní, L., Bejar, M. T., & Badimon, L. (2016). LRP5/canonical Wnt signaling and healing of ischemic myocardium. *Basic Research in Cardiology*, *111*(6), 67. https://doi.org/10.1007/s00395-016-0585-y

Brembeck, F. H., Schwarz-Romond, T., Bakkers, J., Wilhelm, S., Hammerschmidt, M., & Birchmeier, W. (2004). Essential role of BCL9-2 in the switch between β-catenin's adhesive and transcriptional functions. *Genes and Development*, *18*(18), 2225–2230. https://doi.org/10.1101/gad.317604

Bui, A. H., & Waks, J. W. (2018). Risk Stratification of Sudden Cardiac Death After Acute Myocardial Infarction. *The Journal of Innovations in Cardiac Rhythm Management*, *9*(2), 3035. https://doi.org/10.19102/ICRM.2018.090201

Burchfield, J. S., Xie, M., & Hill, J. A. (2013). Pathological ventricular remodeling: Mechanisms: Part 1 of 2. *Circulation*, *128*(4), 388–400. https://doi.org/10.1161/CIRCULATIONAHA.113.001878

Castaño, J., Raurell, I., Piedra, J. A., Miravet, S., Duñach, M., & De Herreros, A. G. (2002). β-catenin N- and C-terminal tails modulate the coordinated binding of adherens junction proteins to β-catenin. *Journal of Biological Chemistry*, *277*(35), 31541–31550. https://doi.org/10.1074/jbc.M204376200

Dajani, R., Fraser, E., Roe, S. M., Yeo, M., Good, V. M., Thompson, V., Dale, T. C., & Pearl, L. H. (2003). Structural basis for recruitment of glycogen synthase kinase 3β to the axin-APC scaffold complex. *EMBO Journal*, *22*(3), 494–501. https://doi.org/10.1093/emboj/cdg068

Daniels, D. L., & Weis, W. I. (2005). β-catenin directly displaces Groucho/TLE repressors from Tcf/Lef in Wnt-mediated transcription activation. *Nature Structural and Molecular Biology*, *12*(4), 364–371. https://doi.org/10.1038/nsmb912

Daskalopoulos, E. P., Hermans, K. C. M., Janssen, B. J. A., & Matthijs Blankesteijn, W. (2013). Targeting the Wnt/frizzled signaling pathway after myocardial infarction: A new tool in the therapeutic toolbox? In *Trends in Cardiovascular Medicine* (Vol. 23, Issue 4, pp. 121–127). Elsevier. https://doi.org/10.1016/j.tcm.2012.09.010

Dawson, K., Aflaki, M., & Nattel, S. (2013). Role of the Wnt-Frizzled system in cardiac pathophysiology: A rapidly developing, poorly understood area with enormous potential. In *Journal of Physiology* (Vol. 591, Issue 6, pp. 1409–1432). Wiley-Blackwell. https://doi.org/10.1113/jphysiol.2012.235382

Deb, A. (2014). Cell-cell interaction in the heart via Wnt/β-catenin pathway after cardiac injury. In *Cardiovascular Research* (Vol. 102, Issue 2, pp. 214–223). Oxford University Press. https://doi.org/10.1093/cvr/cvu054

Duan, J., Gherghe, C., Liu, D., Hamlett, E., Srikantha, L., Rodgers, L., Regan, J. N., Rojas, M., Willis, M., Leask, A., Majesky, M., & Deb, A. (2012). Wnt1/βcatenin injury response activates the epicardium and cardiac fibroblasts to promote cardiac repair. *EMBO Journal*, *31*(2), 429–442. https://doi.org/10.1038/emboj.2011.418

Duan, J., Gherghe, C., Liu, D., Hamlett, E., Srikantha, L., Rodgers, L., Regan, J. N., Rojas, M., Willis, M., Leask, A., Majesky, M., & Deb, A. (2012). Wnt1/βcatenin injury response activates the epicardium and cardiac fibroblasts to promote cardiac repair. *EMBO Journal*, *31*(2), 429–442. https://doi.org/10.1038/emboj.2011.418

Eberhart, C. G., & Argani, P. (2019). Wnt Signaling in Human Development: Beta-Catenin Nuclear Translocation in Fetal Lung, Kidney, Placenta, Capillaries, Adrenal, and Cartilage: *Https://Doi.Org/10.1007/S10024-001-0037-Y*. https://doi.org/10.1007/S10024-001-0037-Y

Fagotto, F., Glück, U., & Gumbiner, B. M. (1998). Nuclear localization signal-independent and importin/karyopherin-independent nuclear import of β-catenin. *Current Biology*, *8*(4), 181–190. https://doi.org/10.1016/s0960-9822(98)70082-x

FE, M., HL, W., AE, B., & ME, J. (1983). Sustained ventricular tachyarrhythmias during the early postinfarction period: electrophysiologic findings and prognosis for survival. *Journal of the American College of Cardiology*, *2*(2), 240–250. https://doi.org/10.1016/S0735-1097(83)80159-4

Gessert, S., & Kühl, M. (2010). The multiple phases and faces of Wnt signaling during cardiac differentiation and development. In *Circulation Research* (Vol. 107, Issue 2, pp. 186–199). Circ Res. https://doi.org/10.1161/CIRCRESAHA.110.221531

Gillers, B. S., Chiplunkar, A., Aly, H., Valenta, T., Basler, K., Christoffels, V. M., Efimov, I. R., Boukens, B. J., & Rentschler, S. (2014). Canonical Wnt signaling regulates atrioventricular junction programming and electrophysiological properties. *Circulation Research*, *116*(3), 398–406. https://doi.org/10.1161/CIRCRESAHA.116.304731

Gomez, C., Özbudak, E. M., Wunderlich, J., Baumann, D., Lewis, J., & Pourquié, O. (2008). Control of segment number in vertebrate embryos. *Nature 2008 454:7202*, *454*(7202), 335–339. https://doi.org/10.1038/nature07020

Gordon, M. D., & Nusse, R. (2006). Wnt signaling: Multiple pathways, multiple receptors, and multiple transcription factors. In *Journal of Biological Chemistry* (Vol. 281, Issue 32, pp. 22429–22433). J Biol Chem. https://doi.org/10.1074/jbc.R600015200

Gorenek, B., Lundqvist, C. B., Terradellas, J. B., Camm, A. J., Hindricks, G., Huber, K., Kirchhof, P., Kuck, K.-H., Kudaiberdieva, G., Lin, T., Raviele, A., Santini, M., Tilz, R. R., Valgimigli, M., Vos, M. A., Vrints, C., & Zeymer, U. (2015). Cardiac arrhythmias in acute coronary syndromes: position paper from the joint EHRA, ACCA, and EAPCI task force. *European Heart Journal: Acute Cardiovascular Care*, *4*(4), 386–386. https://doi.org/10.1177/2048872614550583

Gottardi, C. J., & Gumbiner, B. M. (2004). Distinct molecular forms of β-catenin are targeted to adhesive or transcriptional complexes. *Journal of Cell Biology*, *167*(2), 339–349. https://doi.org/10.1083/jcb.200402153

Gottardi, C. J., & Gumbiner, B. M. (2004). Distinct molecular forms of β-catenin are targeted to adhesive or transcriptional complexes. *Journal of Cell Biology*, *167*(2), 339–349. https://doi.org/10.1083/jcb.200402153

Habas, R., & Dawid, I. B. (2005). Dishevelled and Wnt signaling: Is the nucleus the final frontier? *Journal of Biology*, *4*(1), 2. https://doi.org/10.1186/jbiol22

Hahn, J. Y., Cho, H. J., Bae, J. W., Yuk, H. S., Kim, K. Il, Park, K. W., Koo, B. K., Chae, I. H., Shin, C. S., Oh, B. H., Choi, Y. S., Park, Y. B., & Kim, H. S. (2006). β-catenin overexpression reduces myocardial infarct size through differential effects on cardiomyocytes and cardiac fibroblasts. *Journal of Biological Chemistry*, *281*(41), 30979–30989. https://doi.org/10.1074/jbc.M603916200

Hahn, J. Y., Cho, H. J., Bae, J. W., Yuk, H. S., Kim, K. Il, Park, K. W., Koo, B. K., Chae, I. H., Shin, C. S., Oh, B. H., Choi, Y. S., Park, Y. B., & Kim, H. S. (2006). β-catenin overexpression reduces myocardial infarct size through differential effects on cardiomyocytes and cardiac fibroblasts. *Journal of Biological Chemistry*, *281*(41), 30979–30989. https://doi.org/10.1074/jbc.M603916200

Hamm, C. W., Bassand, J. P., Agewall, S., Bax, J., Boersma, E., Bueno, H., Caso, P., Dudek, D., Gielen, S., Huber, K., Ohman, M., Petrie, M. C., Sonntag, F., Uva, M. S., Storey, R. F., Wijns, W., & Zahger, D. (2011). ESC Guidelines for the management of acute coronary syndromes in patients presenting without persistent ST-segment elevation. In *European Heart Journal* (Vol. 32, Issue 23, pp. 2999–3054). Oxford University Press. https://doi.org/10.1093/eurheartj/ehr236

Hart, M., Concordet, J. P., Lassot, I., Albert, I., Del Los Santos, R., Durand, H., Perret, C., Rubinfeld, B., Margottin, F., Benarous, R., & Polakis, P. (1999). The F-box protein β-TrCP associates with phosphorylated β-catenin and regulates its activity in the cell. *Current Biology*, *9*(4), 207–211. https://doi.org/10.1016/S0960-9822(99)80091-8

Hatsell, S., Rowlands, T., Hiremath, M., & Cowin, P. (2003). β-catenin and Tcfs in Mammary Development and Cancer. In *Journal of Mammary Gland Biology and Neoplasia* (Vol. 8, Issue 2, pp. 145–158). J Mammary Gland Biol Neoplasia. https://doi.org/10.1023/A:1025944723047

He, B. J., Boyden, P., & Scheinman, M. (2018). Ventricular arrhythmias involving the His-Purkinje system in the structurally abnormal heart. In *PACE - Pacing and Clinical Electrophysiology* (Vol. 41, Issue 9, pp. 1051–1059). Blackwell Publishing Inc. https://doi.org/10.1111/pace.13465

He, T. C., Sparks, A. B., Rago, C., Hermeking, H., Zawel, L., Da Costa, L. T., Morin, P. J., Vogelstein, B., & Kinzler, K. W. (1998). Identification of c-MYC as a target of the APC pathway. *Science*, *281*(5382), 1509–1512. https://doi.org/10.1126/science.281.5382.1509

Hohnloser, S. H., Kuck, K. H., Dorian, P., Roberts, R. S., Hampton, J. R., Hatala, R., Fain, E., Gent, M., & Connolly, S. J. (2009). Prophylactic Use of an Implantable Cardioverter–Defibrillator after Acute Myocardial Infarction. *Http://Dx.Doi.Org/10.1056/NEJMoa041489*, *351*(24), 2481–2488. https://doi.org/10.1056/NEJMOA041489

Huang, B., El-Sherif, T., Gidh-Jain, M., Qin, D., & El-Sherif, N. (2001). Alterations of sodium channel kinetics and gene expression in the postinfarction remodeled myocardium. *Journal of Cardiovascular Electrophysiology*, *12*(2), 218–225. https://doi.org/10.1046/j.1540-8167.2001.00218.x

Huber, A. H., Nelson, W. J., & Weis, W. I. (1997). Three-dimensional structure of the armadillo repeat region of β-catenin. *Cell*, *90*(5), 871–882. https://doi.org/10.1016/S0092-8674(00)80352-9

I, N., Y, N., Y, M., Y, M., H, A., A, H., K, K., J, U., S, B., & P, H. (1991). Mutations of chromosome 5q21 genes in FAP and colorectal cancer patients. *Science (New York, N.Y.)*, *253*(5020), 665–669. https://doi.org/10.1126/SCIENCE.1651563

Investigators, T. C. A. S. T. (CAST). (2010). Preliminary Report: Effect of Encainide and Flecainide on Mortality in a Randomized Trial of Arrhythmia Suppression after Myocardial Infarction. *Http://Dx.Doi.Org/10.1056/NEJM198908103210629*, *321*(6), 406–412. https://doi.org/10.1056/NEJM198908103210629

Iyer, L. M., Nagarajan, S., Woelfer, M., Schoger, E., Khadjeh, S., Zafiriou, M. P., Kari, V., Herting, J., Pang, S. T., Weber, T., Rathjens, F. S., Fischer, T. H., Toischer, K., Hasenfuss, G., Noack, C., Johnsen, S. A., & Zelarayán, L. C. (2018). A context-specific cardiac-catenin and GATA4 interaction influences TCF7L2 occupancy and remodels chromatin driving disease progression in the adult heart. *Nucleic Acids Research*, *46*(6), 2850–2867. https://doi.org/10.1093/nar/gky049

Iyer, L. M., Nagarajan, S., Woelfer, M., Schoger, E., Khadjeh, S., Zafiriou, M. P., Kari, V., Herting, J., Pang, S. T., Weber, T., Rathjens, F. S., Fischer, T. H., Toischer, K., Hasenfuss, G., Noack, C., Johnsen, S. A., & Zelarayán, L. C. (2018). A context-specific cardiac-catenin and GATA4 interaction influences TCF7L2 occupancy and remodels chromatin driving disease progression in the adult heart. *Nucleic Acids Research*, *46*(6), 2850–2867. https://doi.org/10.1093/nar/gky049

Janse, M. J., & Wit, A. L. (1989). Electrophysiological mechanisms of ventricular arrhythmias resulting from myocardial ischemia and infarction. *Https://Doi.Org/10.1152/Physrev.1989.69.4.1049*, *69*(4), 1049–1169. https://doi.org/10.1152/PHYSREV.1989.69.4.1049

Janse, M. J., Coronel, R., Wilms-Schopman, F. J. G., & De Groot, J. R. (2003). Mechanical effects on arrhythmogenesis: from pipette to patient. *Progress in Biophysics and Molecular Biology*, *82*(1–3), 187–195. https://doi.org/10.1016/S0079-6107(03)00015-4

Janssen, R., Le Gouar, M., Pechmann, M., Poulin, F., Bolognesi, R., Schwager, E. E., Hopfen, C., Colbourne, J. K., Budd, G. E., Brown, S. J., Prpic, N.-M., Kosiol, C., Vervoort, M., Damen, W. G., Balavoine, G., & McGregor, A. P. (2010). Conservation, loss, and redeployment of Wnt ligands in protostomes: implications for understanding the evolution of segment formation. *BMC Evolutionary Biology 2010 10:1*, *10*(1), 1–21. https://doi.org/10.1186/1471-2148-10-374

JM, D. D., & C, A. (2011). Ischemic ventricular arrhythmias: experimental models and their clinical relevance. *Heart Rhythm*, *8*(12), 1963–1968. https://doi.org/10.1016/J.HRTHM.2011.06.036

Josephson, M. E., Horowitz, L. N., & Farshidi, A. (1978). Continuous local electrical activity. A mechanism of recurrent ventricular tachycardia. *Circulation*, *57*(4), 659–665. https://doi.org/10.1161/01.CIR.57.4.659

Kääb, S., Dixon, J., Duc, J., Ashen, D., Näbauer, M., Beuckelmann, D. J., Steinbeck, G., McKinnon, D., & Tomaselli, G. F. (1998). Molecular basis of transient outward potassium current downregulation in human heart failure: A decrease in Kv4.3 mRNA correlates with

a reduction in current density. *Circulation*, *98*(14), 1383–1393. https://doi.org/10.1161/01.CIR.98.14.1383

Kaidi, A., Williams, A. C., & Paraskeva, C. (2007). Interaction between β-catenin and HIF-1 promotes cellular adaptation to hypoxia. *Nature Cell Biology*, *9*(2), 210–217. https://doi.org/10.1038/ncb1534

Kapoor, N., Liang, W., Marbán, E., & Cho, H. C. (2013). Direct conversion of quiescent cardiomyocytes to pacemaker cells by expression of Tbx18. *Nature Biotechnology*, *31*(1), 54–62. https://doi.org/10.1038/nbt.2465

Kelly, K. F., Ng, D. Y., Jayakumaran, G., Wood, G. A., Koide, H., & Doble, B. W. (2011). β-catenin enhances Oct-4 activity and reinforces pluripotency through a TCF-independent mechanism. *Cell Stem Cell*, *8*(2), 214–227. https://doi.org/10.1016/j.stem.2010.12.010

Komiya, Y., & Habas, R. (2008). Wnt signal transduction pathways. In *Organogenesis* (Vol. 4, Issue 2, pp. 68–75). Landes Bioscience. https://doi.org/10.4161/org.4.2.5851

L, M., J, C., P, B., J, B., J, F., C, B., & J, S.-S. (1996). Predisposing factors and prognostic value of sustained monomorphic ventricular tachycardia in the early phase of acute myocardial infarction. *Journal of the American College of Cardiology*, *28*(7), 1670–1676. https://doi.org/10.1016/S0735-1097(96)00383-X

Li, G., Khandekar, A., Yin, T., Hicks, S. C., Guo, Q., Takahashi, K., Lipovsky, C. E., Brumback, B. D., Rao, P. K., Weinheimer, C. J., & Rentschler, S. L. (2018). Differential Wnt-mediated programming and arrhythmogenesis in right versus left ventricles. *Journal of Molecular and Cellular Cardiology*, *123*, 92–107. https://doi.org/10.1016/j.yjmcc.2018.09.002

Liang, W., Cho, H. C., & Marbán, E. (2015). Wnt signaling suppresses voltage-dependent Na+ channel expression in postnatal rat cardiomyocytes. *Journal of Physiology*, *593*(5), 1147–1157. https://doi.org/10.1113/jphysiol.2014.285551

Libby, P., & Theroux, P. (2005). Pathophysiology of coronary artery disease. In *Circulation* (Vol. 111, Issue 25, pp. 3481–3488). Lippincott Williams & Wilkins. https://doi.org/10.1161/CIRCULATIONAHA.105.537878

Lim, X., Tan, S. H., Koh, W. L. C., Chau, R. M. W., Yan, K. S., Kuo, C. J., Amerongen, R. van, Klein, A. M., & Nusse, R. (2013). Interfollicular Epidermal Stem Cells Self-Renew via Autocrine Wnt Signaling. *Science*, *342*(6163), 1226–1230. https://doi.org/10.1126/SCIENCE.1239730

Liu, C., Li, Y., Semenov, M., Han, C., Baeg, G. H., Tan, Y., Zhang, Z., Lin, X., & He, X. (2002). Control of β-catenin phosphorylation/degradation by a dual-kinase mechanism. *Cell*, *108*(6), 837–847. https://doi.org/10.1016/S0092-8674(02)00685-2

Lyashenko, N., Winter, M., Migliorini, D., Biechele, T., Moon, R. T., & Hartmann, C. (2011). Differential requirement for the dual functions of β-catenin in embryonic stem cell self-renewal and germ layer formation. *Nature Cell Biology 2011 13:7*, *13*(7), 753–761. https://doi.org/10.1038/ncb2260

Malekar, P., Hagenmueller, M., Anyanwu, A., Buss, S., Streit, M. R., Weiss, C. S., Wolf, D., Riffel, J., Bauer, A., Katus, H. A., & Hardt, S. E. (2010). Wnt signaling is critical for maladaptive cardiac hypertrophy and accelerates myocardial remodeling. *Hypertension*, *55*(4), 939–945. https://doi.org/10.1161/HYPERTENSIONAHA.109.141127

Maltsev, V. A., Silverman, N., Sabbah, H. N., & Undrovinas, A. I. (2007). Chronic heart failure slows late sodium current in human and canine ventricular myocytes: Implications for repolarization variability. *European Journal of Heart Failure*, *9*(3), 219–227. https://doi.org/10.1016/j.ejheart.2006.08.007

Mann, B., Gelos, M., Siedow, A., Hanski, M. L., Gratchev, A., Ilyas, M., Bodmer, W. F., Moyer, M. P., Riecken, E. O., Buhr, H. J., & Hanski, C. (1999). Target genes of β-catenin-T cell-factor/lymphoid-enhancer-factor signaling in human colorectal carcinomas. *Proceedings of the National Academy of Sciences of the United States of America*, *96*(4), 1603–1608. https://doi.org/10.1073/pnas.96.4.1603

Mao, J., Wang, J., Liu, B., Pan, W., Farr, G. H., Flynn, C., Yuan, H., Takada, S., Kimelman, D., Li, L., & Wu, D. (2001). Low-density lipoprotein receptor-related protein-5 binds to Axin and regulates the canonical Wnt signaling pathway. *Molecular Cell*, *7*(4), 801–809. https://doi.org/10.1016/S1097-2765(01)00224-6

Mazumdar, J., O'Brien, W. T., Johnson, R. S., Lamanna, J. C., Chavez, J. C., Klein, P. S., & Simon, M. C. (2010). O2 regulates stem cells through Wnt/β-catenin signaling. *Nature Cell Biology*, *12*(10), 1007–1013. https://doi.org/10.1038/ncb2102

Molgat, A. S. D., Tilokee, E. L., Rafatian, G., Vulesevic, B., Ruel, M., Milne, R., Suuronen, E. J., & Davis, D. R. (2014). Hyperglycemia inhibits cardiac stem cell-mediated cardiac repair and angiogenic capacity. *Circulation*, *130*(11), S70–S76. https://doi.org/10.1161/CIRCULATIONAHA.113.007908

Mosimann, C., Hausmann, G., & Basler, K. (2009). β-catenin hits chromatin: Regulation of Wnt target gene activation. In *Nature Reviews Molecular Cell Biology* (Vol. 10, Issue 4, pp. 276–286). Nat Rev Mol Cell Biol. https://doi.org/10.1038/nrm2654

Nakagawa, A., Naito, A. T., Sumida, T., Nomura, S., Shibamoto, M., Higo, T., Okada, K., Sakai, T., Hashimoto, A., Kuramoto, Y., Oka, T., Lee, J. K., Harada, M., Ueda, K., Shiojima, I., Limbourg, F. P., Adams, R. H., Noda, T., Sakata, Y., … Komuro, I. (2016). Activation of endothelial β-catenin signaling induces heart failure. *Scientific Reports*, *6*. https://doi.org/10.1038/srep25009

Niehrs, C. (2010). On growth and form: a Cartesian coordinate system of Wnt and BMP signaling specifies bilaterian body axes. *Development*, *137*(6), 845–857. https://doi.org/10.1242/DEV.039651

Oikonomopoulos, A., Sereti, K. I., Conyers, F., Bauer, M., Liao, A., Guan, J., Crapps, D., Han, J. K., Dong, H., Bayomy, A. F., Fine, G. C., Westerman, K., Biechele, T. L., Moon, R. T., Force, T., & Liao, R. (2011). Wnt signaling exerts an antiproliferative effect on adult cardiac progenitor cells through IGFBP3. *Circulation Research*, *109*(12), 1363–1374. https://doi.org/10.1161/CIRCRESAHA.111.250282

Oikonomopoulos, A., Sereti, K. I., Conyers, F., Bauer, M., Liao, A., Guan, J., Crapps, D., Han, J. K., Dong, H., Bayomy, A. F., Fine, G. C., Westerman, K., Biechele, T. L., Moon, R. T., Force, T., & Liao, R. (2011). Wnt signaling exerts an antiproliferative effect on adult cardiac progenitor cells through IGFBP3. *Circulation Research*, *109*(12), 1363–1374. https://doi.org/10.1161/CIRCRESAHA.111.250282

Oikonomopoulos, A., Sereti, K. I., Conyers, F., Bauer, M., Liao, A., Guan, J., Crapps, D., Han, J. K., Dong, H., Bayomy, A. F., Fine, G. C., Westerman, K., Biechele, T. L., Moon, R. T., Force, T., & Liao, R. (2011). Wnt signaling exerts an antiproliferative effect on adult cardiac progenitor cells through IGFBP3. *Circulation Research*, *109*(12), 1363–1374. https://doi.org/10.1161/CIRCRESAHA.111.250282

Ozhan, G., & Weidinger, G. (2015). Wnt/β-catenin signaling in heart regeneration. *Cell Regeneration*, *4*(1), 4:3. https://doi.org/10.1186/s13619-015-0017-8

Patel, S., Alam, A., Pant, R., & Chattopadhyay, S. (2019). Wnt Signaling and Its Significance Within the Tumor Microenvironment: Novel Therapeutic Insights. In *Frontiers in Immunology* (Vol. 10, p. 2872). Frontiers Media S.A. https://doi.org/10.3389/fimmu.2019.02872

Petersen, C. P., & Reddien, P. W. (2009). Wnt Signaling and the Polarity of the Primary Body Axis. In *Cell* (Vol. 139, Issue 6, pp. 1056–1068). Elsevier B.V. https://doi.org/10.1016/j.cell.2009.11.035

Piedra, J., Miravet, S., Castaño, J., Pálmer, H. G., Heisterkamp, N., García de Herreros, A., & Duñach, M. (2003). p120 Catenin-Associated Fer and Fyn Tyrosine Kinases Regulate β-catenin Tyr-142 Phosphorylation and β-catenin-α-Catenin Interaction. *Molecular and Cellular Biology*, *23*(7), 2287–2297. https://doi.org/10.1128/mcb.23.7.2287-2297.2003

Pitt, G. S., Dun, W., & Boyden, P. A. (2006). Remodeled cardiac calcium channels. In *Journal of Molecular and Cellular Cardiology* (Vol. 41, Issue 3, pp. 373–388). J Mol Cell Cardiol. https://doi.org/10.1016/j.yjmcc.2006.06.071

Pogwizd, S. M., & Corr, P. B. (1990). Mechanisms underlying the development of ventricular fibrillation during early myocardial ischemia. *Circulation Research*, *66*(3), 672–695. https://doi.org/10.1161/01.RES.66.3.672

Pride, Y. B., Appelbaum, E., Lord, E. E., Sloan, S., Cannon, C. P., Sabatine, M. S., & Gibson, C. M. (2009). Relation Between Myocardial Infarct Size and Ventricular Tachyarrhythmia Among Patients With Preserved Left Ventricular Ejection Fraction Following Fibrinolytic Therapy for ST-Segment Elevation Myocardial Infarction. *American Journal of Cardiology*, *104*(4), 475–479. https://doi.org/10.1016/j.amjcard.2009.04.005

Puljevic, D., Smalcelj, A., Durakovic, Z., & Goldner, V. (1998). Effects of postmyocardial infarction scar size, cardiac function, and severity of coronary artery disease on QT interval dispersion as a risk factor for complex ventricular arrhythmia. *PACE - Pacing and Clinical Electrophysiology*, *21*(8), 1508–1516. https://doi.org/10.1111/j.1540-8159.1998.tb00237.x

Reed, G. W., Rossi, J. E., & Cannon, C. P. (2017). Acute myocardial infarction. In *The Lancet* (Vol. 389, Issue 10065, pp. 197–210). Lancet Publishing Group. https://doi.org/10.1016/S0140-6736(16)30677-8

Sekiya, T., & Zaret, K. S. (2007). Repression by Groucho/TLE/Grg Proteins: Genomic Site Recruitment Generates Compacted Chromatin In Vitro and Impairs Activator Binding In Vivo. *Molecular Cell*, *28*(2), 291–303. https://doi.org/10.1016/j.molcel.2007.10.002

Shtutman, M., Zhurinsky, J., Simcha, I., Albanese, C., D'Amico, M., Pestell, R., & Ben-Ze'ev, A. (1999). The cyclin D1 gene is a target of the β-catenin/LEF-1 pathway. *Proceedings of the National Academy of Sciences of the United States of America*, *96*(10), 5522–5527. https://doi.org/10.1073/pnas.96.10.5522

Sierra, J., Yoshida, T., Joazeiro, C. A., & Jones, K. A. (2006). The APC tumor suppressor counteracts β-catenin activation and H3K4 methylation at Wnt target genes. *Genes and Development*, *20*(5), 586–600. https://doi.org/10.1101/gad.1385806

Sinner, D., Rankin, S., Lee, M., & Zorn, A. M. (2004). Sox17 and β-catenin cooperate to regulate the transcription of endodermal genes. *Development*, *131*(13), 3069–3080. https://doi.org/10.1242/dev.01176

Söderholm, S., & Cantù, C. (2020). The WNT/β-catenin dependent transcription: A tissue-specific business. *WIREs Syst Biol Med*. https://doi.org/10.1002/wsbm.1511

Solanas, G., Miravet, S., Casagolda, D., Castaño, J., Raurell, I., Corrionero, A., García De Herreros, A., & Duñach, M. (2004). α-Catenin and plakoglobin N- and C-tails determine ligand specificity. *Journal of Biological Chemistry*, *279*(48), 49849–49856. https://doi.org/10.1074/jbc.M408685200

Spinale, F. G. (2007). Myocardial matrix remodeling and the matrix metalloproteinases: Influence on cardiac form and function. In *Physiological Reviews* (Vol. 87, Issue 4, pp. 1285–1342). American Physiological Society. https://doi.org/10.1152/physrev.00012.2007

Srinivasan, N. T., & Schilling, R. J. (2018). Sudden Cardiac Death and Arrhythmias. *Arrhythmia & Electrophysiology Review*, *7*(2), 111. https://doi.org/10.15420/aer.2018:15:2

Steinbeck, G., Andresen, D., Seidl, K., Brachmann, J., Hoffmann, E., Wojciechowski, D., Kornacewicz-Jach, Z., Sredniawa, B., Lupkovics, G., Hofgärtner, F., Lubinski, A., Rosenqvist, M., Habets, A., Wegscheider, K., & Senges, J. (2009). Defibrillator Implantation Early after Myocardial Infarction. *Http://Dx.Doi.Org/10.1056/NEJMoa0901889*, *361*(15), 1427–1436. https://doi.org/10.1056/NEJMOA0901889

Steinhart, Z., & Angers, S. (2018). Wnt signaling in development and tissue homeostasis. In *Development (Cambridge, England)* (Vol. 145, Issue 11). Oxford University Press for The Company of Biologists Limited. https://doi.org/10.1242/dev.146589

Su, Y. Y., Fu, C., Ishikawa, S., Stella, A., Kojima, M., Shitoh, K., Schreiber, E. M., Day, B. W., & Liu, B. (2008). APC Is Essential for Targeting Phosphorylated β-catenin to the SCFβ-TrCP Ubiquitin Ligase. *Molecular Cell*, *32*(5), 652–661. https://doi.org/10.1016/j.molcel.2008.10.023

Tetsu, O., & McCormick, F. (1999). β-catenin regulates expression of cyclin D1 in colon carcinoma cells. *Nature*, *398*(6726), 422–426. https://doi.org/10.1038/18884

Tsuji, Y., Opthof, T., Kamiya, K., Yasui, K., Liu, W., Lu, Z., & Kodama, I. (2000). Pacing-induced heart failure causes a reduction of delayed rectifier potassium currents along with decreases in calcium and transient outward currents in rabbit ventricle. *Cardiovascular Research*, *48*(2), 300–309. https://doi.org/10.1016/S0008-6363(00)00180-2

Undrovinas, A. I., Maltsev, V. A., & Sabbah, H. N. (1999). Repolarization abnormalities in cardiomyocytes of dogs with chronic heart failure: Role of sustained inward current. *Cellular and Molecular Life Sciences*, *55*(3), 494–505. https://doi.org/10.1007/s000180050306

Wang, B., Zhao, L., Fish, M., Logan, C. Y., & Nusse, R. (2015). Self-renewing diploid Axin2+ cells fuel homeostatic renewal of the liver. *Nature 2015 524:7564*, *524*(7564), 180–185. https://doi.org/10.1038/nature14863

Wang, N., Huo, R., Cai, B., Lu, Y., Ye, B., Li, X., Li, F., & Xu, H. (2016). Activation of Wnt/β-catenin signaling by hydrogen peroxide transcriptionally inhibits NaV1.5 expression. *Free Radical Biology and Medicine*, *96*, 34–44. https://doi.org/10.1016/j.freeradbiomed.2016.04.003

Wang, N. C., Maggioni, A. P., Konstam, M. A., Zannad, F., Krasa, H. B., Burnett, J. C., Grinfeld, L., Swedberg, K., Udelson, J. E., Cook, T., Traver, B., Zimmer, C., Orlandi, C., & Gheorghiade, M. (2008). Clinical implications of QRS duration in patients hospitalized with worsening heart failure and reduced left ventricular ejection fraction. *JAMA - Journal of the American Medical Association*, *299*(22), 2656–2666. https://doi.org/10.1001/jama.299.22.2656

Wang, Y., & Hill, J. A. (2010). Electrophysiological remodeling in heart failure. In *Journal of Molecular and Cellular Cardiology* (Vol. 48, Issue 4, pp. 619–632). NIH Public Access. https://doi.org/10.1016/j.yjmcc.2010.01.009

Wang, Y., & Hill, J. A. (2010). Electrophysiological remodeling in heart failure. In *Journal of Molecular and Cellular Cardiology* (Vol. 48, Issue 4, pp. 619–632). J Mol Cell Cardiol. https://doi.org/10.1016/j.yjmcc.2010.01.009

Willert, K., & Nusse, R. (2012). Wnt proteins. *Cold Spring Harbor Perspectives in Biology*, *4*(9). https://doi.org/10.1101/cshperspect.a007864

Wit, A. L., & Peters, N. S. (2012). The role of gap junctions in the arrhythmias of ischemia and infarction. *Heart Rhythm*, *9*(2), 308–311. https://doi.org/10.1016/j.hrthm.2011.09.056

Wray, J., Kalkan, T., Gomez-Lopez, S., Eckardt, D., Cook, A., Kemler, R., & Smith, A. (2011). Inhibition of glycogen synthase kinase-3 alleviates Tcf3 repression of the pluripotency network and increases embryonic stem cell resistance to differentiation. *Nature Cell Biology*, *13*(7), 838–845. https://doi.org/10.1038/ncb2267

Xing, Y., Clements, W. K., Kimelman, D., & Xu, W. (2003). Crystal structure of a β-catenin/Axin complex suggests a mechanism for the β-catenin destruction complex. *Genes and Development*, *17*(22), 2753–2764. https://doi.org/10.1101/gad.1142603

Xing, Y., Takemaru, K. I., Liu, J., Berndt, J. D., Zheng, J. J., Moon, R. T., & Xu, W. (2008). Crystal Structure of a Full-Length β-catenin. *Structure*, *16*(3), 478–487. https://doi.org/10.1016/j.str.2007.12.021

Ye, Q., Zhang, J., & Ma, L. (2020). Predictors of all-cause 1-year mortality in myocardial infarction patients. *Medicine*, *99*(29), e21288. https://doi.org/10.1097/MD.0000000000021288

Yu, W., Yang, L., Li, T., & Zhang, Y. (2019). Cadherin Signaling in Cancer: Its Functions and Role as a Therapeutic Target. In *Frontiers in Oncology* (Vol. 9, p. 989). Frontiers Media S.A. https://doi.org/10.3389/fonc.2019.00989

Zelarayán, L. C., Noack, C., Sekkali, B., Kmecova, J., Gehrke, C., Renger, A., Zafiriou, M. P., Van Der Nagel, R., Dietz, R., De Windt, L. J., Balligand, J. L., & Bergmann, M. W. (2008). β-catenin downregulation attenuates ischemic cardiac remodeling through enhanced resident precursor cell differentiation. *Proceedings of the National Academy of Sciences of the United States of America*, *105*(50), 19762–19767. https://doi.org/10.1073/pnas.0808393105

Zeng, X., Huang, H., Tamai, K., Zhang, X., Harada, Y., Yokota, C., Almeida, K., Wang, J., Doble, B., Woodgett, J., Wynshaw-Boris, A., Hsieh, J. C., & He, X. (2008). Initiation of Wnt signaling: Control of Wnt coreceptor Lrp6 phosphorylation/activation via frizzled,

dishevelled and axin functions. *Development*, *135*(2), 367–375. https://doi.org/10.1242/dev.013540

Zhang, D., Tu, H., Wadman, M. C., & Li, Y. L. (2018). Substrates and potential therapeutics of ventricular arrhythmias in heart failure. *European Journal of Pharmacology*, *833*, 349–356. https://doi.org/10.1016/j.ejphar.2018.06.024

Zhao, L., Sun, L., Lu, Y., Li, F., & Xu, H. (2019). A small-molecule LF3 abrogates β-catenin/TCF4-mediated suppression of NaV1.5 expression in HL-1 cardiomyocytes. *Journal of Molecular and Cellular Cardiology*, *135*, 90–96. https://doi.org/10.1016/j.yjmcc.2019.08.007